Published in final edited form as:
Development. 2003 November ; 130(22): 5385–5400. doi:10.1242/dev.00770.

Even-skipped, acting as a repressor, regulates axonal projections in *Drosophila*

Miki Fujioka[1], **Bridget C. Lear**[2,*], **Matthias Landgraf**[3], **Galina L. Yusibova**[1], **Jian Zhou**[1], **Kristen M. Riley**[1], **Nipam H. Patel**[2,†], and **James B. Jaynes**[1,‡]

[1]Department of Microbiology and Immunology, Thomas Jefferson University, 1020 Locust Street, Philadelphia, PA 19107, USA

[2]Department of Anatomy and Organismal Biology and HHMI, University of Chicago, MC1028, AMBN101, 5841 South Maryland Avenue, Chicago, IL 60637, USA

[3]Department of Zoology, University of Cambridge, Cambridge CB2 3EJ, UK

Summary

Nervous system-specific *eve* mutants were created by removing regulatory elements from a 16 kb transgene capable of complete rescue of normal *eve* function. When transgenes lacking the regulatory element for either RP2+a/pCC, EL or U/CQ neurons were placed in an *eve*-null background, *eve* expression was completely eliminated in the corresponding neurons, without affecting other aspects of *eve* expression. Many of these transgenic flies were able to survive to fertile adulthood. In the RP2+a/pCC mutant flies: (1) both RP2 and aCC showed abnormal axonal projection patterns, failing to innervate their normal target muscles; (2) the cell bodies of these neurons were positioned abnormally; and (3) in contrast to the wild type, pCC axons often crossed the midline. The Eve HD alone was able to provide a weak, partial rescue of the mutant phenotype, while both the Groucho-dependent and -independent repressor domains contributed equally to full rescue of each aspect of the mutant phenotype. Complete rescue was also obtained with a chimeric protein containing the Eve HD and the Engrailed repressor domain. Consistent with the apparent sufficiency of repressor function, a fusion protein between the Gal4 DNA-binding domain and Eve repressor domains was capable of actively repressing UAS target genes in these neurons. A key target of the repressor function of Eve was *Drosophila Hb9*, the derepression of which correlated with the mutant phenotype in individual *eve*-mutant neurons. Finally, homologues of Eve from diverse species were able to rescue the *eve* mutant phenotype, indicating conservation of both targeting and repression functions in the nervous system.

Keywords

Axon guidance; Homeodomain; Transcriptional repressor; Evx; Hb9; Grunge; Atrophin; Groucho; Eve; Nervous system

‡Author for correspondence (e-mail: E-mail: jaynes@mail.jci.tju.edu).
*Present address: Department of Neurobiology and Physiology, Northwestern University, 2205 Tech Drive #2–160, Evanston, IL 60208, USA
†Present address: Department of Integrative Biology, 3060 VLSB # 3140, University of California, Berkeley, Berkeley, CA 94720-3140, USA

Introduction

The homeobox-containing gene *even skipped* (*eve*) was first identified as a segmentation gene based on the cuticular pattern of hypomorphic mutants (Nüsslein-Volhard and Wieschaus, 1980). In order to function as a segmentation gene, the transcriptional repressor function of the gene product Eve is required, and also appears to be sufficient, in the context of the Eve homeodomain (HD) (Fujioka et al., 1995; Fujioka et al., 2002). The domains of Eve necessary to repress target genes were analyzed in cultured cells (Han and Manley, 1993; Jaynes and O'Farrell, 1991) and in vivo, and two distinct repressor domains were identified. One was shown to be dependent on the co-repressor Groucho (Kobayashi et al., 2001), while the other is Groucho independent (Jimenez et al., 1997), and was shown to interact functionally with the *Drosophila* Atrophin homologue Grunge (Erkner et al., 2002; Zhang et al., 2002). Each of these repressor domains was shown to be required for segmentation function both at the blastoderm stage and early in gastrulation, with each domain contributing roughly equally to the activity on each target gene (Fujioka et al., 2002).

Later during *Drosophila* development, *eve* is expressed in the nervous system, in the mesoderm in cells which develop into dorsal muscles and pericardial cells, and in the anal plate ring (Frasch et al., 1987). Regulatory elements sufficient to drive each of these aspects of the pattern were localized, downstream of the coding region (Fujioka et al., 1999; Sackerson et al., 1999). In the nervous system, Eve is expressed in some ganglion mother cells (GMCs) and in their daughter neurons (Frasch et al., 1987; Patel et al., 1989): the aCC and pCC neurons (derived from GMC 1-1a), the RP2 and RP2-sibling neurons (from GMC 4-2a; *eve* expression in RP2-sibling is subsequently turned off), and the U/CQ neurons (which are generated by several GMCs in the neuroblast 7-1 lineage) (Bossing et al., 1996; Broadus et al., 1995). The other *eve*-expressing neurons, EL neurons, are derived from neuroblast 3–3 (Schmidt et al., 1997); however, the GMCs that produce them are *eve* negative (Skeath and Doe, 1998). The aCC, RP2 and U/CQ neurons are motoneurons, and their axons innervate the dorsal muscle field (Landgraf et al., 1997; Schmid et al., 1999; Sink and Whitington, 1991), whereas the pCC and EL cells are interneurons. Expression of *eve* in the nervous system is well conserved. For example, in the grasshopper *Schistocerca americana* and in Crustaceans, Eve orthologs are expressed in identified neurons that are homologous to those expressing *eve* in *Drosophila* (Duman-Scheel and Patel, 1999; Patel et al., 1992; Patel et al., 1994). Studies of Eve function in the *Drosophila* nervous system using the temperature-sensitive allele eve^{ID19} (also known as eve^{1}) showed that reduced Eve function causes alterations of the RP2 and aCC axonal pathways (Doe et al., 1988), and that the axons of the Eve-positive motoneurons no longer reach the dorsal muscle field (Landgraf et al., 1999). Overexpression of Eve in the nervous system caused a redirection to the dorsal muscle field of axons that normally innervate ventral or lateral muscles, indicating that Eve function is both necessary and sufficient (at least in some contexts) to direct motoneurons to innervate dorsal muscles (Landgraf et al., 1999). In the mouse, expression of the *eve* homologue *evx1* is restricted in the developing spinal cord to V0 interneurons and is not expressed in adjacent V1 interneurons. When *evx1* function was removed, the majority of V0 interneurons failed to extend commissural axons and became similar to V1 neurons, suggesting that Evx1 is a determinant of V0 neuronal identity (Moran-Rivard et al., 2001). Consistent with the action of Eve and its homologues as repressors that use conserved co-repressors, it has been suggested that the pattern of neurogenesis in the mouse neural tube is regulated in part by the spatially controlled repression of transcriptional repressors, through a Groucho/TLE-dependent mechanism (Muhr et al., 2001), while in humans, a mutation (expansion of a polyglutamine tract) in Atrophin is associated with the neurodegenerative disease DRPLA (Koide et al., 1994; Nagafuchi et al., 1994).

Recent studies showed that several HD proteins are involved in the regulation of neuronal identity (Thor and Thomas, 2002). In *Drosophila*, the identities of ventrally projecting

motoneurons appear to be specified by Islet, Lim3 and *Drosophila* Hb9 (Exex – FlyBase), while Eve regulates the identity of dorsally projecting motoneurons (Broihier and Skeath, 2002; Landgraf et al., 1999; Odden et al., 2002; Thor et al., 1999; Thor and Thomas, 1997). The expression patterns of *Drosophila* Hb9 and Eve do not overlap in the wild-type CNS (Broihier and Skeath, 2002; Odden et al., 2002), and ectopic expression of Eve represses *Drosophila* Hb9 expression, indicating that *Drosophila Hb9* might be a direct target of Eve (Broihier and Skeath, 2002). Expression of Islet and Eve is also non-overlapping in the wild-type CNS, and ectopic expression of Eve represses *islet* expression in most motoneurons, although neither the absence of Islet nor its ectopic expression was found to change the *eve* expression pattern (Landgraf et al., 1999; Thor and Thomas, 1997). Lim3 and Eve are co-expressed in the EL neurons, but not in other Eve-positive neurons (Broihier and Skeath, 2002).

In this study, we address aspects of Eve protein function and conservation, and investigate in detail the requirements for *eve* function in the nervous system, by creating *eve* neuron-specific mutants. We accomplish this by rescuing *eve*-null mutants with transgenes containing the entire *eve* locus deleted for individual neuronal regulatory elements. This results in a complete loss of detectable Eve expression in the corresponding neurons, without affecting other aspects of the expression pattern. Combining these with reporter transgenes that specifically mark RP2 and a/pCC, we analyze the mutant phenotype. The lack of Eve causes severe alterations in axonal morphology, among other defects. We find that our constructed mutants have a more severe mutant phenotype than that caused by eve^{ID19}, and so apparently have a more complete loss of *eve* function. Furthermore, in situations of partially penetrant rescue, we observe a strong correlation between a mutant axonal morphology and derepression of *Drosophila* Hb9. We test which domains of Eve are required for rescue, and find that the Eve HD alone can partially rescue some aspects of the mutant phenotype. However, for full rescue, both of the Eve repressor domains are required, and this requirement can be fully supplied by a heterologous repressor domain from Engrailed. Homologues of Eve from species as diverse as the mouse are also able to rescue *eve* function in the developing nervous system.

Materials and methods

Plasmid construction

Wild-type *eve* genomic DNA from either −6.4 to +9.2 kb (EGN92) or −6.4 to +8.6 kb (EGN86) was cloned into a modified pCaSpeR vector, as described previously (Fujioka et al., 1999; Fujioka et al., 2002). Throughout this paper, we refer to the P-element transgenes *P[eve-ΔRP2A]*, *P[eve-ΔRP2B*] and *P[eve-ΔRP2C]* by the abbreviated names Δ*RP2A*, Δ*RP2B* and Δ*RP2C*, respectively. RP2+a/pCC neuronal mutant constructs were made by deleting the following regions from EGN92 (Fig. 1): for Δ*RP2A*, +8.2 (*Cla*I) to +9.2 kb (*Eco*RI); for Δ*RP2B*, +8.0 (*Ple*I) to +9.2 kb; and for Δ*RP2C*, +8.0 (*Ple*I) to +8.6 kb (*Nhe*I). The U/CQ neuronal mutant construct ΔCQ was made by deleting the region +3.5 (*Bgl*II) to +4.0 kb (*Nru*I) from EGN92, and the EL neuronal mutant construct ΔEL was created by deleting the region from +1.9 (*Mlu*I) to +2.6 kb (*Eco*RI) from EGN92.

The first generation of RP2+a/pCC-specific Gal4 drivers was constructed as previously described (Baines et al., 1999). The *eve* 5′ promoter region from −275 (*Sfi*I) to +11 bp (*Xho*I) was fused to a fragment (flanked by *Hin*dIII sites) that includes the Gal4-coding region from plasmid pCEP4-Gal4 (gift from Stefan Thor) followed by the *eve* 3′ region from +1306 (*Bst*UI) to +1917 bp (*Mlu*I). The RP2+a/pCC element from +7.9 (*Eco*RI) to +9.2 kb was placed upstream of this *eve* 5′ promoter and Gal4-coding region. This construct was then modified as follows. A 38 bp multi-cloning sequence upstream of *eve* DNA from +91 to +99 nucleotides, followed by an ATG, was used to replace the yeast *GAL4* translation initiation signal with that of *eve*. In addition, the *eve* 3′ region from +1306 to +1521 (*Kpn*I) was used instead of the +1917

end point. The region from +7.9 to +9.2 kb (to generate RRa-Gal4), or two tandem repeats of the fragment from +7.9 to +8.6 kb (to generate *RN2-Gal4*), was then inserted upstream of this promoter-Gal4-coding region.

A Gal4-Eve fusion protein construct has been described previously (Fujioka et al., 2002). This fusion protein coding region was placed downstream of either two tandem repeats of the RP2 +a/pCC element (the *eve* region from +7.9 to +8.6 kb), two tandem repeats of the U/CQ element (the region from +3.5 to +4.3 kb), or the EL element (the region from +1.9 kb, *Mlu*I, to +3.0 kb). Two reporter UAS constructs were made in order to test the ability of Gal4-Eve to actively repress transcription in vivo. For testing the activity in RP2+a/pCC neurons, the mesodermal element (the region from +5.7, *Sph*I, to +6.7 kb, *Sma*I) and the RP2+a/pCC element (+7.9 to +8.6 kb) were cloned upstream of the *eve* 5′ region from −275 to +99 bp, followed by the EGFP coding sequence (Clontech) and the *eve* 3′ untranslated region from +1306 to +1521 bp, followed by the EL element from +1.9 to +3.5 kb. The UAS sequence, amplified by PCR using as a template the pUAST plasmid (Brand and Perrimon, 1993), was inserted between the mesodermal element and *eve* 5′ promoter. To test the repression activity in U/CQ neurons, the fragment from +1.9 to +4.5 kb (*Bam*HI) was cloned upstream of the *eve* 5′ region from −275 to +166 bp, followed by the *lacZ*-coding region and *eve* 3′ sequences from +1306 to +1521 bp. The UAS sequence was inserted between the regulatory fragment and the *eve* 5′ region.

The constructs for expressing modified versions of Eve, as well as the Eve orthologs Tc-eve and Sa-eve, from a complete rescue transgene, have been described previously (Fujioka et al., 2002). For expressing mouse Evx1, the mesodermal element from +5.7 to +6.7 kb and the RP2 +a/pCC element from +7.9 to +8.6 kb were cloned upstream of the *eve* 5′ region from −275 to +99 bp followed by the ATG of a Flag tag fused to the Evx1-coding sequence and the *eve* 3′ untranslated region from +1306 to +1521 bp. This transgene expresses Evx1 in the mesoderm and in the RP2, aCC and pCC neurons.

Drosophila strains

Transgenic lines were established as described previously (Fujioka et al., 2000; Rubin and Spradling, 1982). When either Δ*RP2A*, Δ*RP2B* or Δ*RP2C* was placed in an *eve*-null mutant background, expression of Eve at the blastoderm stage appeared to be normal. When either the Δ*RP2A* or Δ*RP2B* transgene insertion was homozygous, *engrailed* expression was regularly spaced as in the wild type, indicating that the segmentation function of *eve* was fully rescued (data not shown). However, at the extended germ-band stage, *eve* expression in the mesoderm was often weak or missing in these lines. By contrast, mesodermal expression was normal in the Δ*RP2C*-rescued lines (data not shown). However, in the Δ*RP2C* lines, the odd-numbered parasegments were narrower than normal, indicating a lower activity at the blastoderm stage. Because of this, only one out of five lines with this construct gave rescue to adulthood. When one copy of the Δ*RP2C* transgene was combined (in trans) with one copy of the Δ*RP2A* transgene, mesodermal expression was normal, segmentation was normal and these heterozygotes were efficiently rescued to adulthood. In these rescued embryos, *eve* expression was never observed in RP2 and a/pCC neurons, whereas *eve* expression was normal in EL and U/CQ neurons in all lines (see Results). Unlike some of the RP2-element deletions, deletion of the EL or U/CQ element did not cause a reduction of either mesodermal expression or segmentation function, and both were able to be maintained as stocks. Rescue transgenic lines were crossed into a *Df(2R)eve* mutant background unless otherwise indicated.

In order to mark clearly the axons of RP2, aCC and pCC neurons, we used the RP2 element to express Gal4 (Brand and Perrimon, 1993), and this in turn to drive *UAS-τlacZ*. In our first such attempt using a single copy of the RP2+a/pCC element (from +7.9 to +9.2 kb) upstream of *GAL4* (*GAL4-RRC* and *RRK*), only two out of 40 lines were able to reliably activate UAS reporter gene expression (Baines et al., 1999), and even in these cases, activity was rather weak.

We tested whether this low activity might be due to a lack of efficient translation in the nervous system by changing the translational initiation signal (which was derived from the *GAL4* gene of yeast) to that found in the *eve* gene (see above for details). With this modification, 11 out of 11 lines were able to drive strong UAS reporter expression (data not shown), albeit with some neuromere-to-neuromere variability. We then tested two tandem repeats of the region from +7.9 to +8.6 kb upstream of *GAL4* (*RN2-GAL4*), and found that this drove expression that was more consistently strong in all neuromeres (see Results). *RN2-Gal4* on the third chromosome was recombined with either *UAS-τlacZ* (Callahan et al., 1995) or *UAS-CD8GFP* (Lee and Luo, 1999), and used in this study.

Genetic crosses and analysis of embryos

To analyze GFP expression in the RP2 mutant (described in Results), each of the following four lines was self-crossed: (1) *Df(2R)eve,ΔRP2A/SM6a;RN2-GAL4, UAS-CD8GFP*; (2) *Df(2R)eve, ΔRP2C/SM6a;RN2-GAL4,UAS-CD8GFP*; (3) eve^{R13},*ΔRP2C/SM6a; RN2-GAL4,UAS-CD8GFP*; or (4) *Df(2R)eve,ΔRP2A/*eve^{R13},*ΔRP2C;RN2-GAL4, UAS-CD8GFP/TM3*. In the case of the fourth line, the analyzed population of GFP-expressing progeny contained the following three second chromosome genotypes: *Df(2R)eve,ΔRP2A* homozygotes, eve^{R13},*ΔRP2C* homozygotes, and *Df(2R)eve,ΔRP2A/*eve^{R13},*ΔRP2C*. The subpopulation of these embryos homozygous for the *RN2-GAL4,UAS-CD8GFP* third chromosome (which gave a stronger GFP signal than *RN2-GAL4,UAS-CD8GFP/TM3*) was used for the analysis.

For all experiments using a *CyO* balancer chromosome (below), the progeny not carrying this chromosome (negative for *wg-lacZ* staining) were analyzed. For the rescue experiments with modified Eve proteins, embryos from the following crosses were analyzed. A line carrying

Df(2R)eve,ΔRP2A/CyO,P[wg-lacZ];RN2-GAL4,UAS-τlacZ was crossed with lines of each of the following second and third chromosome genotypes:

for the unrescued control, *Df(2R)eve/CyO,P[wg-lacZ];ΔRP2B*;

for wild-type Eve, *Df(2R)eve,P [EGN86]/CyO,P[wg-lacZ];RN2-GAL4,UAS-τlacZ*;

for tagged wild-type Eve, *Df(2R)eve/CyO,P[wg-lacZ];P[t-WT]*;

for EveH, *Df(2R)eve,P[EveH]/CyO,P[wg-lacZ];P[ΔRP2B]*;

for EveNH, *Df(2R)eve,P[EveNH]/CyO,P[wg-lacZ];P[ΔRP2B]*;

for EveΔC, *Df(2R)eve,P[EveΔC]/CyO,P[wg-lacZ];RN2-GAL4,UAS-τlacZ*;

for EveΔR, *Df(2R)eve,P[EveΔR]/CyO,P[wg-lacZ];RN2-GAL4,UAS-τlacZ*;

for EveH-En, *Df(2R)eve,P[EveH-En]/CyO,P[wg-lacZ];RN2-GAL4,UAS-τlacZ*;

for Tc-eve, *Df(2R)eve,P[Tc-eve]/CyO,P[wg-lacZ];RN2-GAL4, UAS-τlacZ*;

for Sa-eve, *Df(2R)eve,P[Sa-eve]/CyO,P[wg-lacZ];RN2-GAL4,UAS-τlacZ*; and for Evx1, *Df(2R)eve,P[Evx1]/CyO,P[wg-lacZ];P[ΔRP2B]*.

More than 2 lines of each were analyzed, and the lines showing better rescue for each of the constructs were used for further analysis (however, each of the lines examined showed the same overall trends, with only small variations among them). For two-copy rescue by EveΔR and EveΔC, the following lines were used: *Df(2R)eve, P[EveΔR]* (or *P[EveΔC]*)*/CyO,P[wg-lacZ];RN2-GAL4,UAS-τlacZ* was crossed with *Df(2R)eve,P[EveΔR]* (or *P[EveΔC]*)*/CyO,P[wg-lacZ];ΔRP2B*. In all cases, the combination of rescue transgenes provided complete rescue of *eve* segmentation function (data not shown).

For analysis of the temperature-sensitive allele *eve*^{ID19}, *eve*^{ID19}*/CyO,P[wg-lacZ];RN2-GAL4,UAS-τlacZ* was self-crossed for two copies of *eve*^{ID19}, or for one copy, was crossed with *Df(2R)eve,ΔRP2A/CyO,P[wg-lacZ];RN2-GAL4,UAS-τlacZ*. In each case, embryos were collected at 25°C for 1 hour, and were allowed to develop further at 18.5°C for 4 hours. Segmentation was rescued well under these conditions, as determined from analyzing cuticle preparations (Nüsslein-Volhard and Wieschaus, 1980). The embryos were then incubated at 18.5°C (permissive temperature) or 30°C (restrictive temperature), until they developed to the appropriate stages.

Antibody staining was performed as described previously using biotinylated secondary antibodies and SA-HRP (Patel, 1994). The staining was visualized using the HRP-DAB reaction with or without nickel. For immunofluorescent staining, FITC-conjugated anti-mouse (1:1000) and Texas Red-conjugated anti-rabbit (1:500, Jackson ImmunoResearch) secondary antibodies were used. The following primary antibodies were used: polyclonal anti-Eve at 1:10,000, a gift from M. Frasch (Frasch et al., 1987); anti-Eve monoclonal 2B8 (Patel et al., 1994) at 1:20; polyclonal anti-β-gal at 1:200 (ICN); anti-Fas2 monoclonal 1D4 (Vactor et al., 1993) at 1:10; rabbit anti-*Drosophila* Hb9, a gift from J. B. Skeath (Broihier and Skeath, 2002) at 1:500; anti-Futsch monoclonal 22C10 (Fujita et al., 1982) at 1:5; and rat anti-Islet, a gift from J. B. Skeath (Broihier and Skeath, 2002) at 1:200. For the *τlacZ* marker, the following modifications to the published protocol were used: secondary antibody was incubated overnight at 4°C (instead of 1–2 hours at room temperature), and the incubation time for SA-HRP was prolonged to 2 hours (from 1 hour) at room temperature.

Lucifer Yellow injections

Late stage 16 (14 hours 15 minutes±15 minutes) wild-type and RP2 mutant embryos were dissected in Sorensen phosphate buffer as described previously (Landgraf et al., 1997), with the modifications that collagenase treatment was omitted, and dissected embryos were fixed in 3.7% formaldehyde for 20 minutes. Neurons (RP2, aCC, and pCC) were identified by a combination of GFP expression (using *RN2-GAL4;UAS-CD8GFP*) and their position in the nerve cord. Cells were filled with Lucifer Yellow, and preparations were processed, as described previously (Zlatic et al., 2003).

Immunocytochemistry for single-cell labeling

We used the following primary antibodies: anti-Lucifer Yellow (at 1:1000, Molecular Probes), anti-CD8 (at 1:50, Caltag Laboratories) and Cy5-conjugated goat anti-Horseradish Peroxidase (at 1:200, Jackson ImmunoResearch); and secondary antibody Alexa488-conjugated goat anti-rabbit (at 1:500, Molecular Probes). The images shown are maximum projections of confocal *z*-series acquired with a Leica SP confocal microscope and processed with Adobe Photoshop software.

Results

Generation of neuronal cell-type-specific *eve* mutants

A regulatory element capable of driving expression in neurons RP2, aCC and pCC was previously identified in the *eve* locus (Fujioka et al., 1999). We asked whether this region is necessary for expression in the context of a transgene capable of complete functional rescue of *eve* null mutants. This rescue transgene extends from −6.4 to either +8.6 or +9.2 kb, with either end point providing full function when homozygous, at most chromosomal insertion sites (Fujioka et al., 1999; Fujioka et al., 2002). We used a transgene construct with a deletion in the RP2+a/pCC enhancer region to fully rescue segmentation function, while simultaneously removing it from the RP2, aCC and pCC neurons and their progenitors (see Materials and methods). In these rescued embryos, *eve* expression was never observed in RP2 and a/pCC

neurons, while *eve* expression was normal in EL and U/CQ neurons in all lines (Fig. 2C,D, and data not shown). Throughout this paper, this combination of rescuing transgenes in the background of a null mutation at the endogenous *eve* locus is referred to as the RP2 mutant.

Cell-type-specific U/CQ mutant flies were created analogously, by deleting the U/CQ expression element from the full-length rescue construct and placing the resulting transgene in an *eve*-null background. EL mutants were similarly made using a deletion of the EL enhancer (Fig. 1). These deletions resulted in the loss of detectable expression specifically in either U/CQ or EL neurons, respectively (Fig. 2F,G,I,J).

These data indicate that each of the neuronal regulatory elements is not only sufficient, but is also necessary for *eve* expression in the corresponding set of neurons. Somewhat surprisingly, each of these neuronal specific mutants survived to adulthood, and neither mutant adults nor larvae showed any obvious behavioral abnormalities.

eve expression is independent of *eve* function in the nervous system

Although *eve* expression was eliminated in specific subsets of neurons in these transgenic lines, we did not know whether the neurons themselves were eliminated, or whether a change in neuronal cell fate had occurred that might alter the activity of the *eve* neuronal enhancer elements. To test whether *eve* regulatory element activity is affected by the loss of *eve* function, we crossed into these lines additional transgenes in which the regulatory elements directly drive *lacZ* expression (Fujioka et al., 1999). In each case, β-gal expression was able to clearly mark the *eve* mutant cells, showing that *eve* function is not required to maintain the activity of the *eve* neuronal enhancers, and that these neurons still exist without *eve* function (Fig. 2E,H,K).

As we were able to mark the mutant cells in our RP2 mutants, we could analyze the resulting morphological changes in detail. (Note that these mutants lack *eve* expression in RP2, aCC, and pCC neurons.) In order to mark axons more clearly, we used a Gal4 driver transgene with a multimerized enhancer region and a modified translation initiation site (see Materials and methods). We used this Gal4 driver (*RN2-GAL4*) in combination with either *UAS-τlacZ* or *UAS-CD8GFP* to examine the mutant phenotype.

Loss of *eve* function causes aberrant positioning of cell bodies and abnormal axonal morphology

In combination with the modified Gal4 driver, *UAS-τlacZ* generated strong marker expression that was consistent from neuromere to neuromere, and clearly marked individual RP2 and a/pCC axons (Fig. 3A). When this reporter was placed in the RP2 mutant background, β-gal staining revealed several abnormalities (Fig. 3B). RP2 neurons were positioned further posterior than normal, lying almost adjacent to aCC, instead of the normal position intermediate between segmentally reiterated groups of a/pCC neurons (arrows, Fig. 3C,D). The positions of mutant RP2s were also often abnormal laterally (out of line with the a/pCCs) and dorsoventrally (data not shown). By contrast, the positions of a/pCC neurons were more normal, lying just dorsal to the positions of the most medially located U/CQ neurons (Fig. 3D), as in the wild type; however, their positions relative to each other were abnormal (see below).

We analyzed the morphologies of RP2, aCC and pCC in detail using the combination of two labeling methods. In addition to using the *τlacZ* marker (Fig. 3E–P), we used dye injection to anterogradely label single cells in both wild-type and mutant embryos, at late stage 16 (Fig. 4). The RP2 neurons showed the widest range of mutant phenotypes. In the wild type, RP2 axons extend anterolaterally from the cell body, through the posterior root of the intersegmental nerve (pISN; Fig. 3G,I, arrow in Fig. 4A), and out towards the muscle field (Fig. 3E). Dendritic arbors emerge from the proximal axon and extend mainly anteriorly (arrowhead in Fig. 4A)

and, to a somewhat lesser extent, also posteriorly (not shown). In the RP2 mutants, about half of the RP2s extended an axon anteriorly along a lateral longitudinal fascicle, as in the wild type, but the axon failed to exit the CNS and enter the muscle field (arrowhead in Fig. 3H; Fig. 4D; Table 1 'anterior extension, truncated'). The second most commonly observed defect was an axon extending posteriorly and failing to enter the muscle field (arrow in Fig. 3H; Table 1 'posterior extension, truncated'). Some mutant RP2 axons that projected posteriorly did exit the CNS, but via the anterior root of the ISN (aISN; arrow in Fig. 3J; Table 1 'posterior extension') rather than through the normal pISN (arrowhead in Fig. 3J). These posteriorly projecting RP2 axons seemed to occur more often in anterior regions of the CNS, and were not represented among the single-cell labelings. Some mutant RP2s exhibited contralateral axonal projections, mostly through the anterior commissure (Fig. 4C, Table 1 'crossed midline'). Consistent with an abnormal axonal searching behavior, most of the mutant RP2 axons appeared thicker than in the wild type, and the mutant RP2s exhibited many more filopodia (Fig. 3H,J). In addition, about 19% of mutant RP2s appeared to have bipolar axons (Table 1 and Fig. 4C), whereas no RP2s do so in the wild type.

Overall, using the *τlacZ* marker, we found that only 21–23% of RP2 axons extended out of the CNS toward the muscle field (Table 1 'wild-type*' and 'posterior extension' combined; Fig. 3F). Young first instar larvae showed a similar fraction of RP2 axons exiting the CNS (data not shown). Consistent with this, we observed mutant RP2s in embryos by single-cell labeling that had a nearly normal dendritic arbor (arrowheads in Fig. 4B) and which projected an axon in the normal direction, anteriorly into the pISN root (arrow in Fig. 4B). Out of the 23 RP2s labeled with this technique, eight were observed with these characteristics (Fig. 4B). Of these eight, two had axons that remained within the CNS, while the axons of the remaining six exited the CNS via the ISN, but did not project to their normal targets. In four out of these six cases, the mutant axon terminated within the ventral ISN (not the nerve branch ISNb, the axons of which innervate ventral muscles), while in only two cases were muscles contacted, and these were ventral muscles (ventral oblique muscles 4–6) rather than the normal dorsal muscles (data not shown). This essentially complete failure to extend to the normal target region, the dorsal muscle field, was confirmed with the CD8GFP reporter, as described below.

In the wild type, aCC neurons extend their axons posteroperipherally through the aISN and have predominantly anteriorly projecting dendrites (Fig. 3E, Fig. 4E) (Landgraf et al., 1997;Schmid et al., 1999;Sink and Whitington, 1991). In the mutant, virtually all aCC neurons showed clear abnormalities (Table 2; Fig. 3F,H,J, Fig. 4F,G). Many aCCs extended short axons anteriorly or posteriorly that usually seemed to attach to RP2 axons. Some aCC axons were also observed to cross the midline, mostly at the posterior commissure (Fig. 4F). Unlike the RP2s, one-third of aCCs had no axon (Table 2), and by stage 16, some of these cells appeared to be fragmenting, possibly as part of a cell death process (data not shown). We were able to label only two mutant aCC neurons by intracellular injection. Both had very abnormal morphologies: axons did not exit the CNS, and only one was bipolar (Fig. 4F,G).

The pCC cells are interneurons that extend axons anteriorly (arrow in Fig. 3M and Fig. 4H), and, like aCC and RP2, their axons normally do not cross the midline (Fig. 3K,M, Fig. 4H). However, in the mutant, although pCC axons extended anteriorly along a medial longitudinal fascicle as in the wild type, more than one-third of them crossed the midline at the next anterior commissure (Table 3; Fig. 3D,L,N). Single-cell fills of pCC confirmed this phenotype (Fig. 4J), although this technique revealed a smaller fraction of axons crossing the midline, probably owing to the much smaller sample size (Fig. 4; Table 3).

The aCC and pCC neurons are sibling cells that normally exhibit a consistent relative position at stage 12 (Fig. 3O). In the wild type, pCC is located either directly posterior or posterior and slightly lateral to its aCC sibling (Fig. 3O). In the mutant, the relative position of aCC and pCC

appears to be random (Fig. 3P). This mislocation of relative cell body position was also seen to persist through later embryonic stages (Fig. 3B,F,L, and data not shown). At least at later stages, this seems largely to reflect an abnormal position of aCC relative to the neuropile as a whole (data not shown).

In order to test whether our cell-specific mutants have residual *eve* function, we compared our observed phenotypes with those of the previously studied temperature-sensitive allele eve^{ID19} (Doe et al., 1988; Landgraf et al., 1999). Compared with our RP2 mutant, eve^{ID19} (at the restrictive temperature) exhibited more RP2 and aCC neurons extending axons toward the muscle field in almost every segment, and fewer pCC axons crossing the midline (Fig. 3Q). We also crossed these mutants to generate transheterozygotes of eve^{ID19} and Δ*RP2A*. Their phenotype was intermediate between that of our RP2 mutants and that of eve^{ID19} homozygotes (Fig. 3R). These data show that, even though eve^{ID19} exhibits cuticle (segmentation) defects very similar to those of *eve* nulls, it has residual function in the nervous system, while our mutant has less (if any) such residual function.

Even in wild-type embryos, we were not able to use the *τlacZ* marker to follow the axons to the dorsal muscle field. However, we were able to do so using UAS-CD8GFP, and we were also able to clearly visualize neuromuscular junctions (Fig. 5A–D,G,H). When this marker was placed in the RP2 mutant background, although axons were strongly marked in the CNS (Fig. 5B), only a few were observed in the muscle field. About a third of embryos examined showed none (17 out of 50), while most of the remainder showed one or two axons extending outside the CNS. However, there were a few embryos (three out of 50) that had short axons outside the CNS in almost all segments, although these were never seen to reach the dorsal muscle field. In total, axons were observed in the muscle field in 19% of hemisegments (n=366), consistent with the data obtained using *τlacZ* (21–23%, see above) and single-cell labeling (six out of 23). For those axons observed in the muscle field, the GFP intensity was weak relative to that in eve^{+} embryos. This is also consistent with our results described above using the *τlacZ* marker, which showed almost no aCC axons exiting the CNS, so that we would expect only one axon to be present at each position (from RP2) rather than the wild-type combination of two in each hemisegment (from RP2 and aCC). When embryos were stained with anti-Fas2, sites of contact to DA2 (also known as muscle 2), a normal target muscle of both RP2 and U/CQ (Landgraf et al., 1997; Schmid et al., 1999; Sink and Whitington, 1991) and DO2 (a.k.a. muscle 10), a normal target muscle of U/CQ (Landgraf et al., 1997; Schmid et al., 1999) were visible in the mutants, although they were possibly less extensive than in the wild type (arrowheads in Fig. 5I–L), perhaps reflecting the lack of RP2 axons. However, contacts with DA1 muscles (also known as muscle 1), normal targets of aCC (Landgraf et al., 1997; Schmid et al., 1999; Sink and Whitington, 1991) were just barely visible in the mutant (arrows in Fig. 5K,L; compared with the wild type in Fig. 5I,J). The apparent residual innervation beyond the DA2/DO2 neuromuscular junction may be due to U/CQ neurons targeting the DO1 muscle (Schmid et al., 1999).

Eve functions in neurons to repress target genes

At the blastoderm stage, Eve uses two repressor domains to repress target genes. In addition to a generic repression activity, only the HD (with conserved flanking region) is required for Eve function during segmentation (Fujioka et al., 2002). We examined whether the function of Eve is also as a repressor in the nervous system using a series of rescue transgenes expressing modified Eve proteins. In these experiments, one copy of each modified Eve transgene was used to rescue nervous system function (in RP2, aCC and pCC), in the background of the RP2 mutant (see Materials and methods for details). Single copies of these transgenes were compared in order to allow clearer distinctions to be made among them, as we found that a single copy of the wild-type construct could provide almost complete rescue (see below). The

resulting rescued axonal phenotypes are summarized in Table 1–Table 3. As described earlier, in the RP2 mutant alone, about 12% of RP2 axons and 2% of aCC axons exited the CNS via the normal route, while 60% of pCC axons showed a normal phenotype (Table 1–Table 3, Fig. 6A). When one copy of the wild-type rescue transgene was combined with the mutant, almost all (97%) RP2 axons, and 100% of aCC and pCC axons, showed a normal phenotype (Table 1–Table 3; Fig. 6F). When a Flag-tagged wild-type protein was used as an additional control (as modified proteins carried such a tag) the percentage of rescue was reduced slightly in RP2 and aCC (Table 1 and Table 2). When the Eve HD alone was supplied to these neurons, there was some rescue of both RP2 and pCC (EveH; Table 1–Table 3, Fig. 6B), but not of aCC. When the N terminus of the protein was added to the HD, there was some additional rescue of pCC (EveNH; Table 3, Fig. 6C). In addition to rescuing axonal morphology, EveNH also showed some degree of rescue of the RP2 position, as well as the relative positions of the aCC and pCC cell bodies (Fig. 6C). When either of the repressor domains alone was added to the EveNH construct, rescue of both the RP2 and aCC axonal phenotypes were substantially increased, and rescue of pCC reached 100% (EveΔC, EveΔR; Table 1–Table 3, Fig. 6D,E). Thus, both repressor domains contribute about equally to the activity of Eve in these neurons. Consistent with this, two copies of either the EveΔR or the EveΔC transgene were sufficient to fully rescue the phenotypes in the nervous system (data not shown). Importantly, the function of the Eve repressor domains could be completely replaced by a heterologous repressor region from the Engrailed protein (EveH-En; Table 1–Table 3, Fig. 6G). Taken together, these data strongly suggest that the Eve HD (with conserved flanking region) is sufficient to recognize correct target genes in the nervous system, and that in addition, active repression function is required. Furthermore, the fact that the HD by itself is able to rescue axonal morphology to varying degrees in different neurons suggests that there may be distinct target genes or mechanisms involved in Eve function in these different neuronal cell types.

Eve homologues are able to function in the *Drosophila* nervous system

To test the extent to which these functions that are required in the nervous system have been conserved during evolution, Eve homologues from several species were tested for rescuing activity in this system. In previous studies, Eve homologues from the red flour beetle (*Tribolium castaneum* Tc-eve), grasshopper (*Schistocerca americana* Sa-eve) and mouse (Evx1) all showed substantial activity during *D. melanogaster* segmentation (Fujioka et al., 2002). These same proteins were analyzed in RP2 mutant embryos in the same way as were the modified Eve proteins described above. All three were able to rescue the mutant phenotype essentially completely in both RP2 and pCC (Table 1, Table 3; Fig. 6H,I,J). In aCC, both Tc-eve and Sa-eve were able to rescue as well as did the *Drosophila* protein, while the activity of Evx1, although detectably weaker, was nonetheless very substantial (Table 2; Fig. 6H,I,J). As such rescue requires both the HD and a strong repressor activity, these data suggest that both targeting to and repression of specific target genes have been conserved in the function of these proteins during nervous system development.

Eve can act as a direct repressor in RP2 and a/pCC

Whether Eve acts as a transcriptional repressor of direct endogenous target genes in these neurons could not be addressed extensively, as the target genes in this tissue are only beginning to be identified. Therefore, we tested whether a chimeric protein of the Gal4 DNA-binding domain fused with the Eve repressor domains (Fujioka et al., 2002) could repress an activated UAS-containing target gene in these cells. Expression of such a transgene in RP2 and a/pCC, as well as in EL neurons to provide an internal control (Fig. 7A), was monitored in the presence or absence of Gal4-EveRC, expressed from a transgene specifically in RP2 and a/pCC (but not ELs). We found that the reporter GFP expression was clearly reduced in both RP2 and a/pCC neurons in the presence of Gal4-EveRC, indicating that Eve can, indeed, act as a direct transcriptional repressor in these cells (Fig. 7B,C). Using a similar strategy, we found that Eve

can also act as a direct repressor in U/CQ neurons (Fig. 7D,E). However, we were not able to detect repressor activity clearly in EL neurons using a similar assay (data not shown).

Derepression of *Drosophila* Hb9 correlates with *eve* mutant phenotypes in RP2 and aCC

The expression of the *Drosophila* Hb9 has previously been shown to be non-overlapping with that of Eve in the CNS (Broihier and Skeath, 2002; Odden et al., 2002). Furthermore, ectopic expression of Eve repressed *Drosophila Hb9* gene expression (also known as *extra-extra*), and expression of *Drosophila* Hb9 was found to be derepressed in RP2 and in either aCC or pCC (which could not be reliably distinguished) in eve^{ID19} and in EveΔC embryos (Broihier and Skeath, 2002). In that study, segmentation was only partially rescued, as Eve activity during segmentation was also reduced, owing to the lack of the Groucho interaction domain in the rescuing EveΔC protein (Kobayashi et al., 2001). Therefore, we examined *Drosophila* Hb9 expression in our neuron-specific mutants. We found that in RP2 mutants rescued by a wild-type transgene, Hb9 was absent from neurons that showed a normal phenotype (e.g., green arrow, Fig. 8A), which represented the great majority, as described above. However, in the minority of RP2 neurons that exhibited an abnormal axonal morphology, such as those extending axons posteriorly (black arrows, Fig. 8A), Hb9 was often detectably derepressed. In the RP2 mutant itself, Hb9 was largely derepressed both in RP2 (black arrows, Fig. 8B) and in aCC (yellow arrow, Fig. 8B). However, derepression of Hb9 in pCC neurons was never observed.

When the EveH transgene was used to rescue the RP2 mutant, expression of Hb9 was often absent or reduced in RP2 neurons relative to the mutant (green arrow, Fig. 8C), although not always (black arrow, Fig. 8C), consistent with the partial rescue of the RP2 mutant phenotype by this protein. In aCC, Hb9 was almost always strongly derepressed (yellow arrow, Fig. 8C), consistent with the inability of this protein to rescue the phenotype of aCC (Table 2). When the RP2 mutant was partially rescued using EveΔC, the degree to which Hb9 was repressed in aCC and RP2 neurons similarly correlated with the degree of their phenotypic rescue: the expression of Hb9 was usually repressed only in those aCC and RP2 neurons with a normal axonal morphology (aCC – yellow arrows, RP2 – black arrows in Fig. 8D). We also obtained very similar results for EveΔR-rescued embryos (data not shown). Thus, overall in these rescued lines, there is a strong correlation between abnormal axonal phenotypes and the derepression of Hb9. However, on a cell-by-cell basis, the correlation is not 100%. In particular, although we observed that neurons with abnormal axons almost always showed derepression of Hb9, a few of those with normal axons also had detectable derepression, although it was never very strong.

The monoclonal antibody 22C10 (Fujita et al., 1982) recognizes a subset of neurons, including RP2 (green arrows, Fig. 8E–H) and aCC (yellow arrow, Fig. 8E,F), but not pCC. This antibody was recently shown to recognize the *futsch* gene product, which is homologous to vertebrate MAP1B, a microtubule-associated protein (Hummel et al., 2000). We used this antibody to examine expression of the antigen in our mutants. We found that although it was still detectable in the RP2 mutant, its expression was weaker than in the wild type, especially in aCC neurons (23 out of 24 neurons showed decreased intensity; yellow arrow, Fig. 8G,H), indicating that it is a downstream target of Eve regulation. We also examined expression of the transcription factor Islet, which is known to be involved in axonal guidance (Thor and Thomas, 1997). However, we did not observe clear derepression in the RP2 mutant (data not shown).

Discussion

Testing the cell-specific requirements for *eve* function in the nervous system

In this study, we created transgenic embryos that lack detectable *eve* expression in specific sets of neurons by deleting individual neuronal regulatory elements from a complete rescue transgene (Fig. 1). These deleted rescue transgenes were placed in the background of an *eve* deficiency mutant that is both a protein and transcript null. In such embryos, *eve* segmentation function can be completely rescued, providing a true neuron-specific *eve* mutant (Fig. 5). Importantly, we found in our analysis that eve^{ID19}, a temperature-sensitive allele that has been used previously to examine *eve* function at later developmental stages, has residual activity in the nervous system (see below), so that the phenotype of our mutant is closer to that of an *eve* null.

The mutants that we constructed lack all detectable Eve expression either in the combination of RP2 and a/pCC neurons, or in the U/CQ neurons, or in the EL neurons (Fig. 2), and here we analyzed in detail the defects in the first of these. In this case, despite significant defects in axonal architecture (discussed below), individuals were able to survive to fertile adulthood. In a preliminary analysis, we did not observe any behavioral abnormalities in either larvae or adult flies (M.F. and J.B.J., unpublished). Eve is normally also expressed in the parental GMCs of RP2, aCC, pCC and the U/CQ neurons, and this expression is also eliminated in our mutants. The removal of Eve from these neuronal lineages did not cause a loss of neurons (Fig. 2), showing that *eve* function in the GMCs is not required for their normal cell division to occur.

In order to identify the mutant neurons and to analyze the axonal phenotypes, the *eve* neuronal elements were used to drive marker gene expression. Expression in RP2+a/pCC was enhanced using the Gal4-UAS system (Brand and Perrimon, 1993). In order to be effective, we found that Gal4 activity needed to be increased by replacing the yeast translational initiation signal in the Gal4 driver transgene with that from *eve*, and by multimerizing the enhancer (see Materials and methods). With these modifications, in combination with a *UAS-τlacZ* transgene (Callahan et al., 1995), the axons of RP2, aCC and pCC were clearly marked (Fig 3, Fig 6 and Fig 8). Combining the same Gal4 driver with *UAS-CD8GFP* (Lee and Luo, 1999) allowed us to mark axons with membrane-localized GFP. This allowed us to examine how far mutant axons grew towards the muscle field, and to visualize connections to specific target muscles (Fig. 5).

The regulation of *eve* neuronal elements

The locations of individual neuronal regulatory elements sufficient for *eve* expression in subsets of neurons were identified previously (Fujioka et al., 1999). Because deleting each of these regulatory elements in the context of the rescue transgene eliminates *eve* expression in the corresponding neurons, the elements are also necessary in the context of the entire gene (Fig. 2), as was found for the *eve* mesodermal enhancer (Han et al., 2002).

In the absence of *eve* function, all neuronal enhancer elements remain active. This suggests that the cells do not completely change their identities in the absence of Eve, but continue to express the combination of factors that normally initiate and maintain *eve* expression, and which presumably act in concert with Eve to specify the phenotype.

Requirements for Eve in RP2 motoneurons

Using a combination of the constructed cell-specific mutant and the marker transgenes described above, we analyzed the morphology of RP2 mutant neurons. The mutant RP2s exhibit a variety of defects in axonal morphology (Fig 3 and Fig 4, summarized in Table 1), and in addition they are defective in their ability to migrate to their normal position within the

CNS (Fig. 2E, Fig. 3). Although the abnormal position of mutant RP2s might affect their ability to extend axons normally, it does not seem to be a primary determinant of whether they extend to the muscle field, because the position defect is often rescued by the Eve protein without its repressor domains (EveNH, supplied by an additional rescue transgene expressing this protein; Fig. 6C), and yet in this case, axons still fail to extend properly. In addition, there are a few abnormally located RP2s in wild-type embryos, and they still extend their axons normally (data not shown). The mutant RP2s seem to retain some axonal guidance capability, as their axons often recognize their normal point of exit from the CNS along the ISN, once they 'happen' onto it, although many of these fail to extend further (Fig 3–Fig 5, Table 1). The RP2 mutant axons were never observed to extend as far as their normal target muscles, and indeed, many of them do not exit the CNS (Fig. 5). Of those that do exit the CNS, most appear to be unable to defasciculate from the ISN onto muscle targets. It is unlikely that the failure of mutant RP2 axons to exit the CNS by stage 16 is due solely to a delay in either axon outgrowth or recognition of the nerve roots, because we find similar percentages of peripherally projecting RP2 neurons in both stage 16 embryos and young first instar larvae.

The inability of the mutant axons to reach the muscle field was partially rescued by the Eve HD without its repressor domains (Fig. 6B,C). However, in addition to the HD, the two distinct repressor domains of Eve contribute strongly to rescue of the mutant phenotype (Fig. 6D,E). Interestingly, complete rescue can also be provided by the Eve HD fused with a heterologous repressor domain from Engrailed (Fig. 6G). Therefore, in addition to the functions provided by the DNA-binding HD, a generic repressor function of sufficient strength is required for normal function in these neurons. The fact that the HD alone can provide a detectable degree of rescue, which contrasts with the lack of its ability to rescue segmentation function (Fujioka et al., 2002), suggests that perhaps competition for binding sites with activators of downstream target genes plays a more prominent role in Eve function in the nervous system. Consistent with the requirement for its repressor domains, an Eve-Gal4 fusion protein was able to actively repress a UAS-containing target gene in RP2 neurons (Fig. 7B,C).

Requirements in aCC motoneurons

The requirement for Eve in axonal guidance is somewhat more stringent in aCC than in RP2 neurons. Although a significant fraction of mutant RP2s initially extend axons in the same direction as wild-type RP2s, essentially none of mutant aCCs do so (Table 2). In addition, unlike for RP2s, the aCC phenotype was not significantly rescued by either the HD alone or the HD with the N terminus (which provides no detectable repression activity, but might stabilize the protein). In aCC, as in RP2, the phenotype was partially rescued by including either repressor domain, and the Engrailed repressor domain was able to provide full activity (Fig. 6). Furthermore, Eve repressor domains were able to actively repress a UAS target gene in aCC neurons (Fig. 7). These data indicate that the primary function of *eve* in aCC is to actively repress target genes. The more stringent requirements in aCC versus RP2 suggest that there may be different target genes in these two motoneurons, although *Drosophila Hb9* is a common target (discussed below).

Requirements in the interneuron pCC

In mutant pCC neurons, in contrast to the wild type, 40% of axons crossed the ventral midline to the contralateral side (Table 3). This phenotype was rescued quite effectively by the HD alone, suggesting that the target gene(s) involved may be passively repressed through a competition for activator binding sites (although more complex possibilities cannot be ruled out). Recent studies have shown that midline crossing is regulated by a complex interplay of responses to attractive and repellent signals secreted by midline cells (reviewed by Dickson, 2002). One possibility is that the midline crossing phenotype of mutant pCCs might be caused

by derepression of the DCC/Frazzled receptor (Kolodziej et al., 1996) for the midline attractant Netrins (Harris et al., 1996;Mitchell et al., 1996).

In addition to the defects in axonal morphology, the cell body position of pCC relative to that of its sibling aCC is apparently randomized in the mutant (Fig. 3P). We do not know whether this is due to the lack of Eve in aCC, in pCC, or in both. As other neurons in the CNS are wild type, it is unlikely to be an effect involving surrounding neurons. This defect is rescued effectively only when the Eve HD is accompanied by at least one repressor domain. It is unclear whether the normally tight control of this characteristic has a role in the subsequent morphogenesis of the neurons.

Null and hypomorphic neuronal phenotypes

Previous studies using the *eve* temperature-sensitive allele eve^{ID19} showed that *eve* is required in *eve*-positive motoneurons for proper axonal morphology, including the ability to reach the dorsal muscle field (Doe et al., 1988; Landgraf et al., 1999). The eve^{ID19} allele contains a point mutation in the HD (Frasch et al., 1988), and shows a near-null segmentation phenotype at the restrictive temperature (Nüsslein-Volhard et al., 1985). However, our data indicate that eve^{ID19} is not a true null in the nervous system (Fig. 3). This might explain the differences between the morphological phenotypes of mutant RP2, aCC and pCC neurons that we observe in our mutant as compared with those seen in eve^{ID19} (Doe et al., 1988).

A significant variation in phenotype with a small change in the level of function is consistent with an interpretation wherein loss of Eve leads to the absence of a particular subset of neuronal properties. Interestingly, even in our mutant, which has no detectable Eve expression in these lineages, some RP2s as well as some pCCs show several of the characteristics of their wild-type counterparts. If we assume that our mutant represents the complete null phenotype, this indicates that, to a limited extent, Eve acts in parallel with other factors in the specification of these cell types, rather than being an overall determinant of the cell fate. This notion is also consistent with the fact that the *eve* regulatory elements, which are specific markers for these cell types, continue to be active in the absence of *eve* function.

Evolutionary conservation of function

A single copy of a wild-type transgene was sufficient to almost completely rescue the mutant phenotypes in the nervous system, in contrast to the requirement for two copies to rescue segmentation (Fujioka et al., 1999). This relative lack of *eve* dosage sensitivity in the nervous system might be related to the apparently ancestral nature and greater conservation of the nervous system function of *eve*.

We tested the extent to which Eve homologues from *Tribolium*, grasshopper, and mouse could rescue the mutant neuronal phenotypes. We found that a single copy of either of the insect orthologs could provide essentially complete function in *Drosophila*, while mouse Evx1 also showed quite strong rescuing capability. Coupled with the fact that active repression function is required for this degree of rescue, these results indicate that each of these homologues has retained both the ability to be targeted to and to repress the key direct target genes of Eve in the nervous system.

Target genes in the nervous system

It has previously been shown that *Drosophila* Hb9 and Eve are expressed in a non-overlapping pattern in the wild-type CNS (Broihier and Skeath, 2002; Odden et al., 2002), and that ectopic Eve expression represses *Hb9*, indicating that *Hb9* is a target gene of Eve (Broihier and Skeath, 2002). We found that *Hb9* is derepressed in the RP2 mutant in both RP2 and aCC (Fig. 8), but not in pCC neurons (the RP2 mutant lacks Eve in all three cell types), showing that there are

significant differences in target gene regulation in different neurons, even in those derived from the same GMC (in the case of aCC and pCC).

When the Eve HD alone is used to rescue the RP2 mutant, Hb9 is repressed in many of the RP2 neurons, and this seemingly stochastic repression correlates with a more normal axonal morphology. However, effective repression, particularly in aCC, requires active repression domains, with either of the repressor domains of Eve alone providing partial activity (in the context of the Eve HD). Although there is a strong correlation in situations of partial rescue between the axonal phenotypes of individual neurons and derepression of Hb9, this correlation is not 100%. This suggests that there may be other key target genes that mediate Eve neuronal function in addition to Hb9. We also found that the level of expression of the antigen (Futsch) of the monoclonal antibody 22C10 (Hummel et al., 2000) is reduced in RP2 and aCC in the absence of Eve (Fig. 8). However, the gene encoding this antigen is likely to be an indirect target of Eve, because its expression is activated rather than repressed by Eve.

Either of the repressor domains of Eve is sufficient to give a similar degree of partial rescue of each of the phenotypes we have studied in the nervous system, including the repression of *Hb9*, showing that these repressor domains provide a similar function. In fact, two copies of a transgene expressing either EveΔC or EveΔR are able to rescue to a similar degree as that of one copy of the wild-type transgene (data not shown). Thus, we see that the recruitment of either of two apparently distinct co-repressors, Groucho or Atrophin, produces the same net result. The two are used in these neurons in an additive fashion to generate the appropriate level of Eve repressor activity, with no apparent target gene specificity.

Acknowledgments

We thank C. Q. Doe, M. Frasch, C. S. Goodman, J. B. Skeath, S. Thor, E. Pym, R. Baines, the Developmental Studies Hybridoma Bank at the University of Iowa and the Bloomington Stock Center for reagents. We also thank Alice Schmid for assistance and helpful discussions, and Caroline Devereux and Yukiko Emi-Sarker for excellent technical assistance. M.L. is funded by a Royal Society Research Fellowship and was also supported by a grant from the Wellcome Trust to Michael Bate. N.H.P. is an Investigator of the Howard Hughes Medical Institute. This work was supported by NIH (GM50231) and NSF (0110856) awards to J.B.J.

References

Baines RA, Robinson SG, Fujioka M, Jaynes JB, Bate M. Postsynaptic expression of tetanus toxin light chain blocks synaptogenesis in *Drosophila*. Curr. Biol 1999;9:1267–1270. [PubMed: 10556094]

Bossing T, Udolph G, Doe CQ, Technau GM. The embryonic central nervous system lineages of *Drosophila melanogaster*. I. Neuroblast lineages derived from the ventral half of the neuroectoderm. Dev. Biol 1996;179:41–64. [PubMed: 8873753]

Brand AH, Perrimon N. Targeted gene expression as a means of altering cell fates and generating dominant phenotypes. Development 1993;118:401–415. [PubMed: 8223268]

Broadus J, Skeath JB, Spana EP, Bossing T, Technau G, Doe CQ. New neuroblast markers and the origin of the aCC/pCC neurons in the *Drosophila* central nervous system. Mech. Dev 1995;53:393–402. [PubMed: 8645605]

Broihier HT, Skeath JB. *Drosophila* homeodomain protein dHb9 directs neuronal fate via crossrepressive and cell-nonautonomous mechanisms. Neuron 2002;35:39–50. [PubMed: 12123607]

Callahan CA, Muralidhar MG, Lundgren SE, Scully AL, Thomas JB. Control of neuronal pathway selection by a *Drosophila* receptor protein-tyrosine kinase family member. Nature 1995;376:171–174. [PubMed: 7603568]

Dickson BJ. Molecular mechanisms of axon guidance. Science 2002;298:1959–1964. [PubMed: 12471249]

Doe CQ, Smouse D, Goodman CS. Control of neuronal fate by the *Drosophila* segmentation gene *even-skipped*. Nature 1988;333:376–378. [PubMed: 3374572]

Duman-Scheel M, Patel NH. Analysis of molecular marker expression reveals neuronal homology n distantly related arthropods. Development 1999;126:2327–2334. [PubMed: 10225992]

Erkner A, Roure A, Charroux B, Delaage M, Holway N, Core N, Vola C, Angelats C, Pages F, Fasano L, et al. Grunge, related to human Atrophin-like proteins, has multiple functions in *Drosophila* development. Development 2002;129:1119–1129. [PubMed: 11874908]

Frasch M, Hoey T, Rushlow C, Doyle H, Levine M. Characterization and localization of the even-skipped protein of *Drosophila*. EMBO J 1987;6:749–759. [PubMed: 2884106]

Frasch M, Warrior R, Tugwood J, Levine M. Molecular analysis of *even-skipped* mutants in *Drosophila* development. Genes Dev 1988;2:1824–1838. [PubMed: 2907321]

Fujioka M, Jaynes JB, Goto T. Early *even-skipped* stripes act as morphogenetic gradients at the single cell level to establish *engrailed* expression. Development 1995;121:4371–4382. [PubMed: 8575337]

Fujioka M, Emi-Sarker Y, Yusibova GL, Goto T, Jaynes JB. Analysis of an *even-skipped* rescue transgene reveals both composite and discrete neuronal and early blastoderm enhancers, and multi-stripe positioning by gap gene repressor gradients. Development 1999;126:2527–2538. [PubMed: 10226011]

Fujioka M, Jaynes JB, Bejsovec A, Weir M. Production of transgenic *Drosophila*. Methods Mol. Biol 2000;136:353–363. [PubMed: 10840724]

Fujioka M, Yusibova GL, Patel NH, Brown SJ, Jaynes JB. The repressor activity of Even-skipped is highly conserved, and is sufficient to activate *engrailed* and to regulate both the spacing and stability of parasegment boundaries. Development 2002;129:4411–4421. [PubMed: 12223400]

Fujita SC, Zipursky SL, Benzer S, Ferrus A, Shotwell SL. Monoclonal antibodies against the *Drosophila* nervous system. Proc. Natl. Acad. Sci. USA 1982;79:7929–7933. [PubMed: 6818557]

Han K, Manley JL. Transcriptional repression by the *Drosophila* even-skipped protein: definition of a minimal repression domain. Genes Dev 1993;7:491–503. [PubMed: 8095483]

Han Z, Fujioka M, Su M, Liu M, Jaynes JB, Bodmer R. Transcriptional integration of competence modulated by mutual repression generates cell-type specificity within the cardiogenic mesoderm. Dev. Biol 2002;252:225–240. [PubMed: 12482712]

Harris R, Sabatelli LM, Seeger MA. Guidance cues at the *Drosophila* CNS midline: identification and characterization of two *Drosophila* Netrin/UNC-6 homologs. Neuron 1996;17:217–228. [PubMed: 8780646]

Hummel T, Krukkert K, Roos J, Davis G, Klambt C. *Drosophila* Futsch/22C10 is a MAP1B-like protein required for dendritic and axonal development. Neuron 2000;26:357–370. [PubMed: 10839355]

Jaynes JB, O′Farrell PH. Active repression of transcription by the engrailed homeodomain protein. EMBO J 1991;10:1427–1433. [PubMed: 1673924]

Jimenez G, Paroush Z, Ish-Horowicz D. Groucho acts as a corepressor for a subset of negative regulators, including Hairy and Engrailed. Genes Dev 1997;11:3072–3082. [PubMed: 9367988]

Kobayashi M, Goldstein RE, Fujioka M, Paroush Z, Jaynes JB. Groucho augments the repression of multiple Even-skipped target genes in establishing parasegment boundaries. Development 2001;128:1805–1815. [PubMed: 11311161]

Koide R, Ikeuchi T, Onodera O, Tanaka H, Igarashi S, Endo K, Takahashi H, Kondo R, Ishikawa A, Hayashi T, et al. Unstable expansion of CAG repeat in hereditary dentatorubral-pallidoluysian atrophy (DRPLA). Nat. Genet 1994;6:9–13. [PubMed: 8136840]

Kolodziej PA, Timpe LC, Mitchell KJ, Fried SR, Goodman CS, Jan LY, Jan YN. *frazzled* encodes a *Drosophila* member of the DCC immunoglobulin subfamily and is required for CNS and motor axon guidance. Cell 1996;87:197–204. [PubMed: 8861904]

Landgraf M, Bossing T, Technau GM, Bate M. The origin, location, and projections of the embryonic abdominal motorneurons of *Drosophila*. J. Neurosci 1997;17:9642–9655. [PubMed: 9391019]

Landgraf M, Roy S, Prokop A, VijayRaghavan K, Bate M. *even-skipped* determines the dorsal growth of motor axons in *Drosophila*. Neuron 1999;22:43–52. [PubMed: 10027288]

Lee T, Luo L. Mosaic analysis with a repressible cell marker for studies of gene function in neuronal morphogenesis. Neuron 1999;22:451–461. [PubMed: 10197526]

Mitchell KJ, Doyle JL, Serafini T, Kennedy TE, Tessier-Lavigne M, Goodman CS, Dickson BJ. Genetic analysis of *Netrin* genes in *Drosophila*: Netrins guide CNS commissural axons and peripheral motor axons. Neuron 1996;17:203–215. [PubMed: 8780645]

Moran-Rivard L, Kagawa T, Saueressig H, Gross MK, Burrill J, Goulding M. Evx1 is a postmitotic determinant of v0 interneuron identity in the spinal cord. Neuron 2001;29:385–399. [PubMed: 11239430]

Muhr J, Andersson E, Persson M, Jessell TM, Ericson J. Groucho-mediated transcriptional repression establishes progenitor cell pattern and neuronal fate in the ventral neural tube. Cell 2001;104:861–873. [PubMed: 11290324]

Nagafuchi S, Yanagisawa H, Ohsaki E, Shirayama T, Tadokoro K, Inoue T, Yamada M. Structure and expression of the gene responsible for the triplet repeat disorder, dentatorubral and pallidoluysian atrophy (DRPLA). Nat. Genet 1994;8:177–182. [PubMed: 7842016]

Nüsslein-Volhard C, Wieschaus E. Mutations affecting segment number and polarity in *Drosophila*. Nature 1980;287:795–801. [PubMed: 6776413]

Nüsslein-Volhard C, Kluding H, Jurgens G. Genes affecting the segmental subdivision of of the *Drosophila* embryo. Cold Spring Harb. Symp. Quant. Biol 1985;50:145–154. [PubMed: 3868475]

Odden JP, Holbrook S, Doe CQ. *Drosophila* HB9 is expressed in a subset of motoneurons and interneurons, where it regulates gene expression and axon pathfinding. J. Neurosci 2002;22:9143–9149. [PubMed: 12417636]

Patel, NH. Imaging neuronal subsets and other cell types in whole mount *Drosophila* embryos and larvae using antibody probes. In: Goldstein, LSB.; Fyrberg, E., editors. Methods in Cell Biology. Vol. Vol. 44. New York: Academic Press; 1994. p. 445-487.

Patel NH, Schafer B, Goodman CS, Holmgren R. The role of segment polarity genes during *Drosophila* neurogenesis. Genes Dev 1989;3:890–904. [PubMed: 2501154]

Patel NH, Ball EE, Goodman CS. Changing role of *even-skipped* during the evolution of insect pattern formation. Nature 1992;357:339–342. [PubMed: 1350328]

Patel NH, Condron BG, Zinn K. Pair-rule expression patterns of *even-skipped* are found in both short- and long-germ beetles. Nature 1994;367:429–434. [PubMed: 8107801]

Rubin GM, Spradling AC. Genetic transformation of *Drosophila* with transposable element vectors. Science 1982;218:348–353. [PubMed: 6289436]

Sackerson C, Fujioka M, Goto T. The *even-skipped* locus is contained in a 16-kb chromatin domain. Dev. Biol 1999;211:39–52. [PubMed: 10373303]

Schmid A, Chiba A, Doe CQ. Clonal analysis of *Drosophila* embryonic neuroblasts: neural cell types, axon projections and muscle targets. Development 1999;126:4653–4689. [PubMed: 10518486]

Schmidt H, Rickert C, Bossing T, Vef O, Urban J, Technau GM. The embryonic central nervous system lineages of *Drosophila melanogaster*. II. Neuroblast lineages derived from the dorsal part of the neuroectoderm. Dev. Biol 1997;189:186–204. [PubMed: 9299113]

Sink H, Whitington PM. Location and connectivity of abdominal motoneurons in the embryo and larva of *Drosophila melanogaster*. J. Neurobiol 1991;22:298–311. [PubMed: 1909747]

Skeath JB, Doe CQ. Sanpodo and Notch act in opposition to Numb to distinguish sibling neuron fates in the *Drosophila* CNS. Development 1998;125:1857–1865. [PubMed: 9550718]

Thor S, Thomas JB. The *Drosophila islet* gene governs axon pathfinding and neurotransmitter identity. Neuron 1997;18:397–409. [PubMed: 9115734]

Thor S, Thomas J. Motor neuron specification in worms, flies and mice: conserved and 'lost' mechanisms. Curr. Opin. Genet. Dev 2002;12:558–564. [PubMed: 12200161]

Thor S, Andersson SG, Tomlinson A, Thomas JB. A LIM-homeodomain combinatorial code for motor-neuron pathway selection. Nature 1999;397:76–80. [PubMed: 9892357]

Vactor DV, Sink H, Fambrough D, Tsoo R, Goodman CS. Genes that control neuromuscular specificity in *Drosophila*. Cell 1993;73:1137–1153. [PubMed: 8513498]

Zhang S, Xu L, Lee J, Xu T. *Drosophila* Atrophin homolog functions as a transcriptional corepressor in multiple developmental processes. Cell 2002;108:45–56. [PubMed: 11792320]

Zlatic M, Landgraf M, Bate M. Genetic specification of axonal arbors: *atonal* regulates *robo3* to position terminal branches in the *Drosophila* nervous system. Neuron 2003;37:41–51. [PubMed: 12526771]

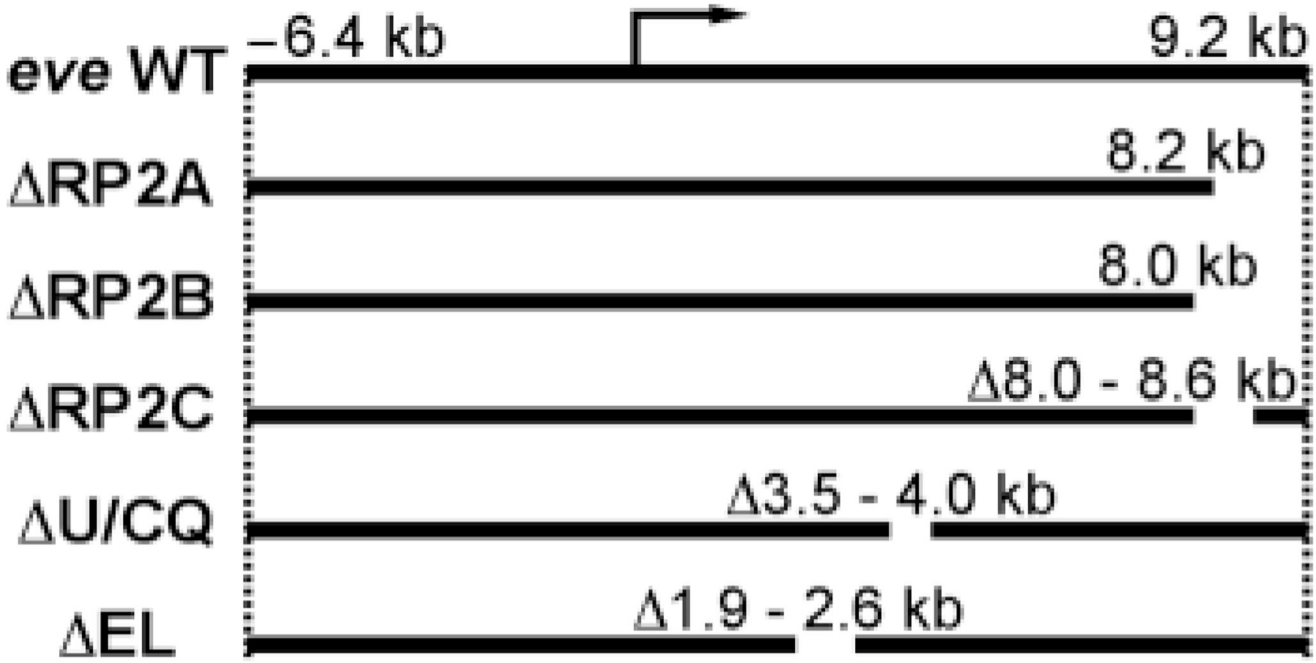

Fig. 1.

Rescue transgenes used to create neuron-specific *eve* mutants. Deletions were made in the context of a complete rescue transgene consisting of the *eve* locus from −6.4 to +9.2 kb (relative to the transcription start site, see Materials and methods for details). Three different deletions (ΔRP2A, B, C) were made in the region sufficient to drive expression in RP2, aCC and pCC neurons. Other deletions were of the minimal elements necessary to drive expression in either U/CQ neurons (ΔU/CQ) or EL neurons (ΔEL). An unbroken line indicates the region included in each construct, while a gap indicates the deleted region. The end points of each deletion are given above the line.

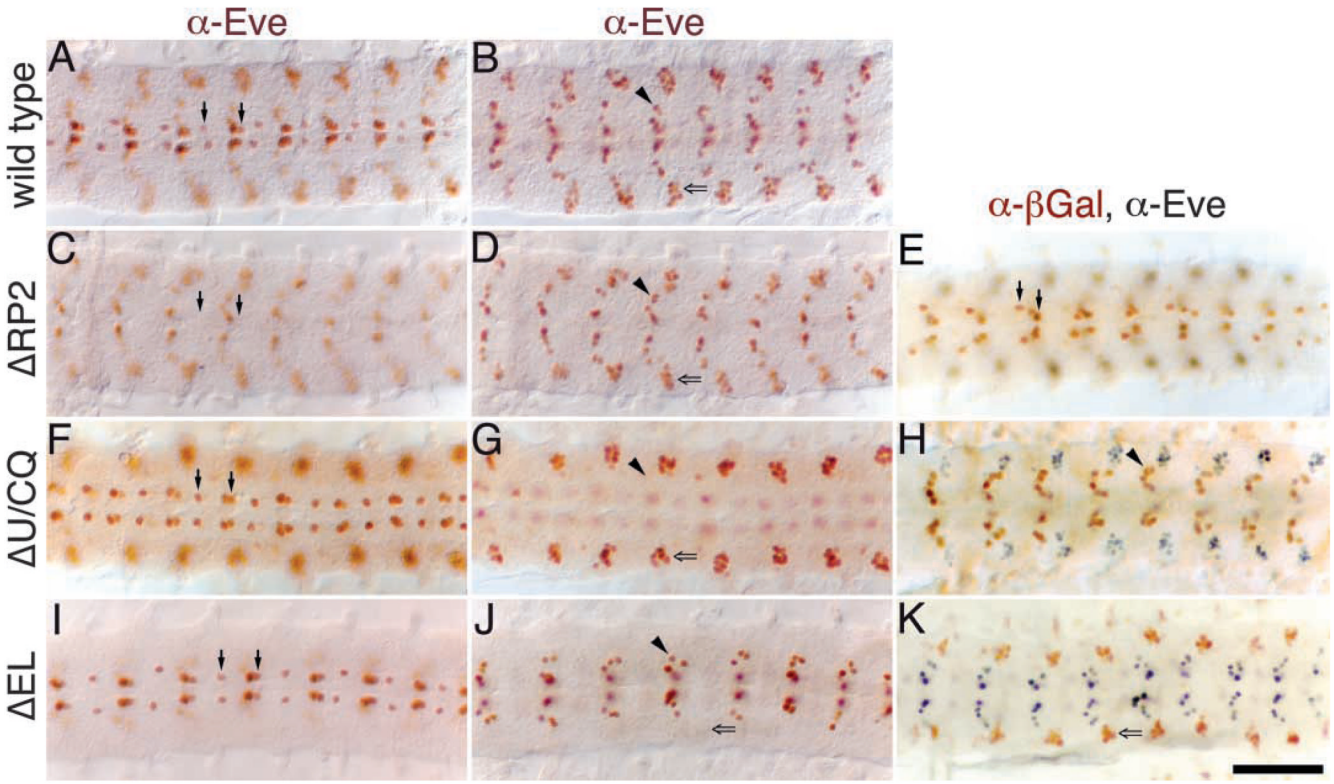

Fig. 2.

Deletion of individual neuronal regulatory elements eliminates expression in the corresponding neurons, without eliminating expression of a reporter driven by the same element. All embryos are in a *Df(2R)eve* mutant background, and carry the rescue transgene indicated on the left of each row (see Fig. 1 and text for details). All are oriented with anterior towards the left. Two different focal planes of the same embryo, stained with anti-Eve, are shown in the first two columns: the focal plane of the RP2 and a/pCC neurons in A,C,F,I; and that of the EL and U/CQ neurons in B,D,G,J. In all panels, black arrows indicate the positions of RP2 (left arrow) and pCC (right arrow) neurons, arrowheads indicate the positions of U/CQ neurons, and open arrows indicate the positions of EL neurons. (A,B) Eve expression from the complete ('wild type') rescue construct. (C,D) Eve expression from ΔRP2A. Note that there is no detectable Eve expression in RP2 and a/pCC neurons. The positions of RP2 and pCC, which do not overlap with those of U/CQ neurons, are indicated by arrows; aCC is also negative for Eve staining, but its position, immediately anterior to pCC, overlaps with that of a U/CQ, which is just out of focus in C. Eve expression in U/CQ (arrowhead) and EL neurons (open arrow) is normal. (E) β -Gal expression (brown) driven by the RP2+a/pCC regulatory element in the same neurons where Eve is missing. Note that the element is still active in the absence of Eve (there is no black anti-Eve staining visible in this focal plane). (F,G) Eve expression from ΔU/CQ. (H) β -gal expression (brown) driven by the U/CQ element in the *eve*$^{-}$ neurons, and Eve expression (black) from ΔU/CQ. (I,J) Eve expression from ΔEL. (K) β -gal expression (brown) driven by the EL element in the *eve*$^{-}$ neurons, and Eve expression from ΔEL (black). Scale bar: 50 μm.

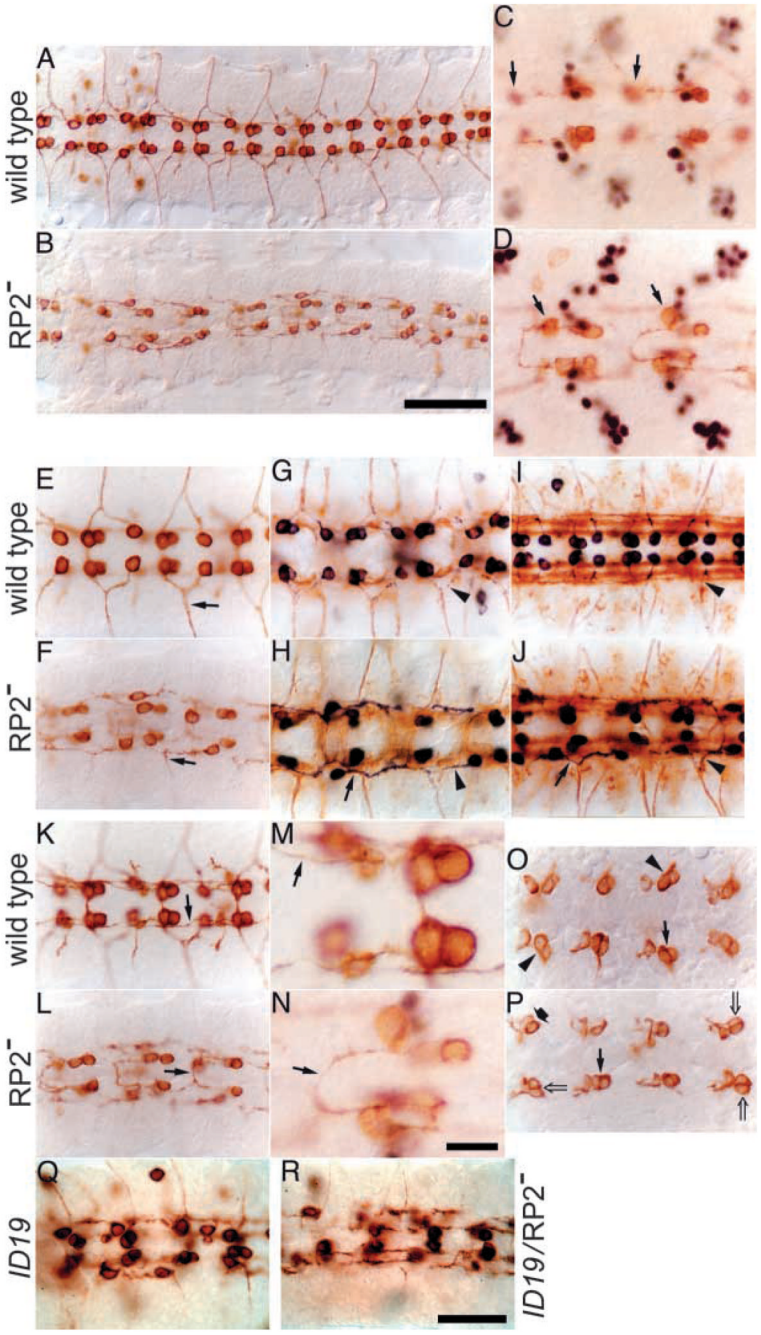

Fig. 3.

Without Eve, RP2 and a/pCC neurons show abnormal axonal morphologies. CNS preparations from embryos carrying both transgenes *UAS-τlacZ* (microtubule-associated βgal marker) and *RN2-Gal4* (RP2+a/pCC driver), in a wild-type background (A,C,E,G,I,K,M,O), a ARP2A mutant background (*eve* null rescued with RP2 element-deleted transgenes; B,D,F,H,J,L,N,P), in an eve^{ID19} background (Q) or in eve^{ID19}, ΔRP2A transheterozygotes (R), as indicated beside each row. (A,B) Anti-β-gal staining; overview of the CNS. Scale bar (in B): 50 μm. (C,D) Anti-Eve staining (black) followed by anti-β-gal staining (brown); black arrows indicate RP2 neurons. The focal plane is that of the U/CQ neurons, so that the RP2s are slightly out of focus. Note that RP2 is abnormally close to aCC in the mutant. (E,F) Anti-β-gal staining; higher

magnification view of A,B in the RP2 and aCC axonal focal plane. Note that very few RP2 axons turn laterally (arrows) in the mutant. (G–J) Anti-β-gal staining (black) followed by anti-Fas2 staining (1D4 antibody, brown); stage 13 (G,H) and stage 15 (I,J) are shown. In the mutant, RP2s often extend an axon posteriorly, rather than anteriorly as in the wild type, along the lateral longitudinal fascicle (arrow in H,J). Although the majority of RP2s extend an axon anteriorly, which then either turns laterally at the pISN (arrowhead in J), as in the wild type, or fails to turn at the ISN (arrowhead in H; compare with the wild type in G,I), most of them do not exit the CNS (see Table 1). Even those that do exit the CNS fail to extend to the dorsal muscle field (see Fig. 5). (K,L) Anti-β-gal staining; higher magnification view of A, B in the pCC axonal focal plane. The pCC axons extend anteriorly beyond the next more anterior pCC cell body in the wild type, while in the mutant, the pCC axons often cross the midline at the anterior commissure (arrows). Note that there are small neurons extending their axons laterally in the wild type. These are RP2 siblings, because at earlier stages, they also stain for Eve (not shown). (M,N) Higher magnification of K and D, respectively. Scale bar (in N): 5 μm. (O,P) Anti-β-gal staining; stage 12 CNSs are shown. In the wild type, the positions of the aCC and pCC cell bodies (after their generation from GMC1-1a) are well regulated; pCC is positioned either posteriorly (arrow) or posteriorly and laterally (arrowheads) relative to aCC. This positioning is disarrayed in the mutant; pCCs positioned posteromedially (wide arrow) or directly laterally (open arrows) are indicated. (Q,R) Anti-β-gal staining; the temperature-sensitive *eve* allele *ID19* kept at the restrictive temperature during nervous system development after allowing segmentation to occur at the permissive temperature (see Materials and methods for details). (Q) eve^{ID19} homozygous mutant; note that many more axons extend laterally than in ΔRP2A/ΔRP2A (compare with F), indicating that eve^{ID19} does not act as a complete null allele in the nervous system. (R) A single copy of eve^{ID19} with one copy of ΔRP2A; note that the phenotype is more severe than that of eve^{ID19} homozygotes (Q) and less severe than that of ΔRP2A/ΔRP2A (F): fewer pCC axons crossed the midline and more axons turned laterally than in F. Scale bar (same size as that in B): 20 μm in C,D; 30 μm in all other panels except A,B,M,N.

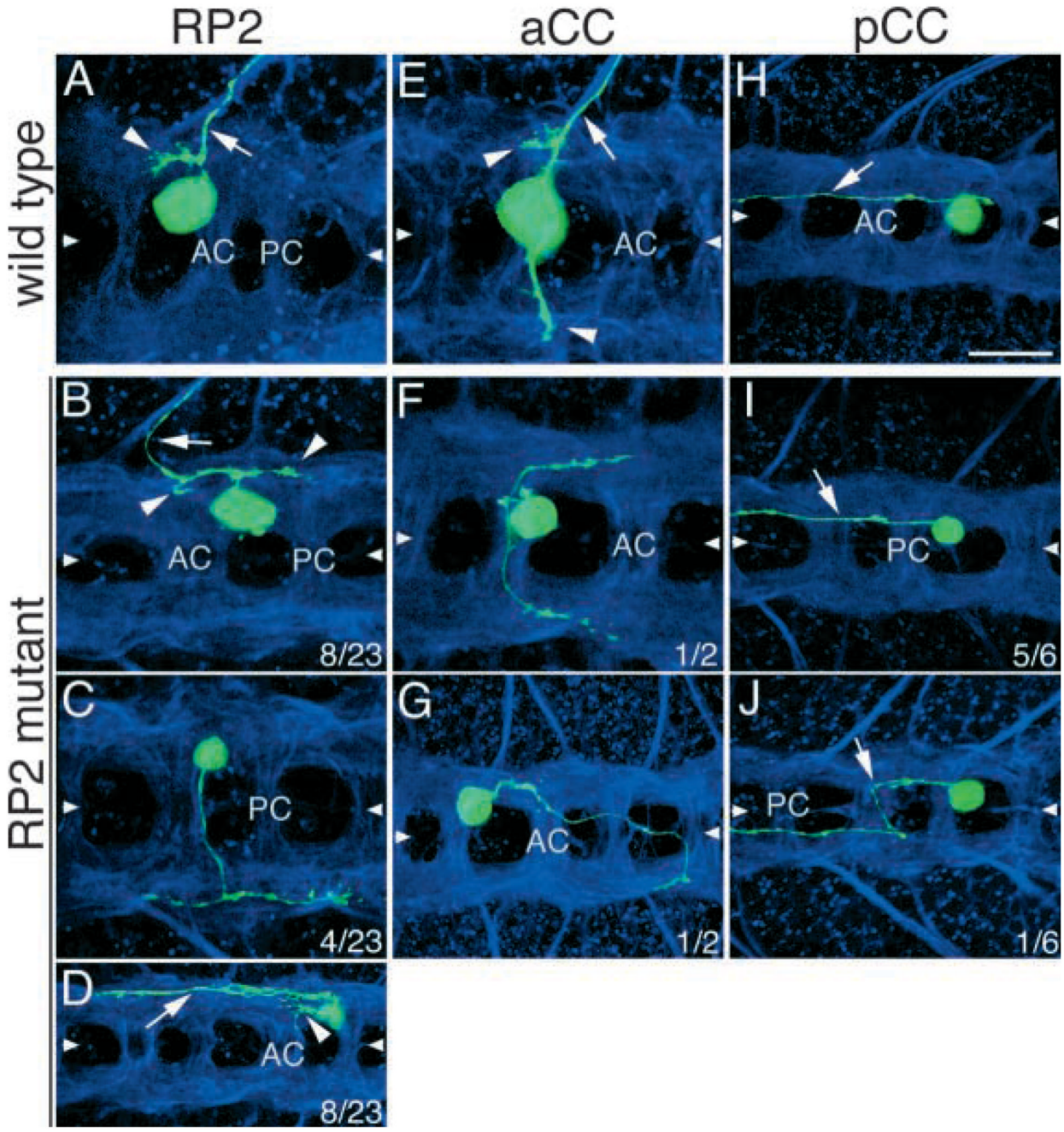

Fig. 4.

Single-cell labelings of wild-type and mutant RP2, aCC and pCC neurons. RP2, aCC and pCC neurons (green) were anterogradely labeled (using Lucifer Yellow) in late stage 16 wild-type (A,E,H) and RP2 mutant (B-D,F,G,I,J) embryos. The neuropile was visualized with anti-HRP antibodies and is shown in blue. (A) In the wild type, the RP2 cell body is normally located medially on the anterior part of the anterior commissure. The RP2 axon exits the CNS via the pISN (arrow). Dendritic arbors (arrowhead) emerge from the proximal axon, mainly anteriorly, but frequently also, although to a lesser extent, posteriorly (not shown here). (B–D) Three of the most frequent morphological classes of mutant RP2 neurons exhibiting (B) relatively normal morphology with axon (arrow) exiting the CNS via the pISN and with dendritic arbors

(arrowheads); (C) contralateral axonal projection; (D) anterior axonal (arrow) and dendritic (arrowhead) projections. (E) Axons (arrow) of wild-type aCC neurons exit via the aISN. Dendrites (arrowhead) extend from the proximal axon mostly anteriorly as well as contralaterally through the posterior commissure. (F,G) Two examples of mutant aCC neurons: axons fail to exit the CNS; the neuron in F still reflects the normal bipolar geometry of aCC. (H) Wild-type pCC neurons extend their axons (arrow) anteriorly for many segments along a medial fascicle. (I,J) Most mutant pCC neurons are relatively wild-type in appearance (I), although a fraction shows midline crossing in the next anterior commissure (J, arrow). All images are projections of confocal *z*-stacks. Anterior is towards the left. Triangles indicate the ventral midline, 'AC' the anterior and 'PC' the posterior commissure. Numbers indicate the fraction of labeled cells in the morphological class represented by the images. Scale bar: 10 μm in A–C,E,F; 16 μm in D,G–J.

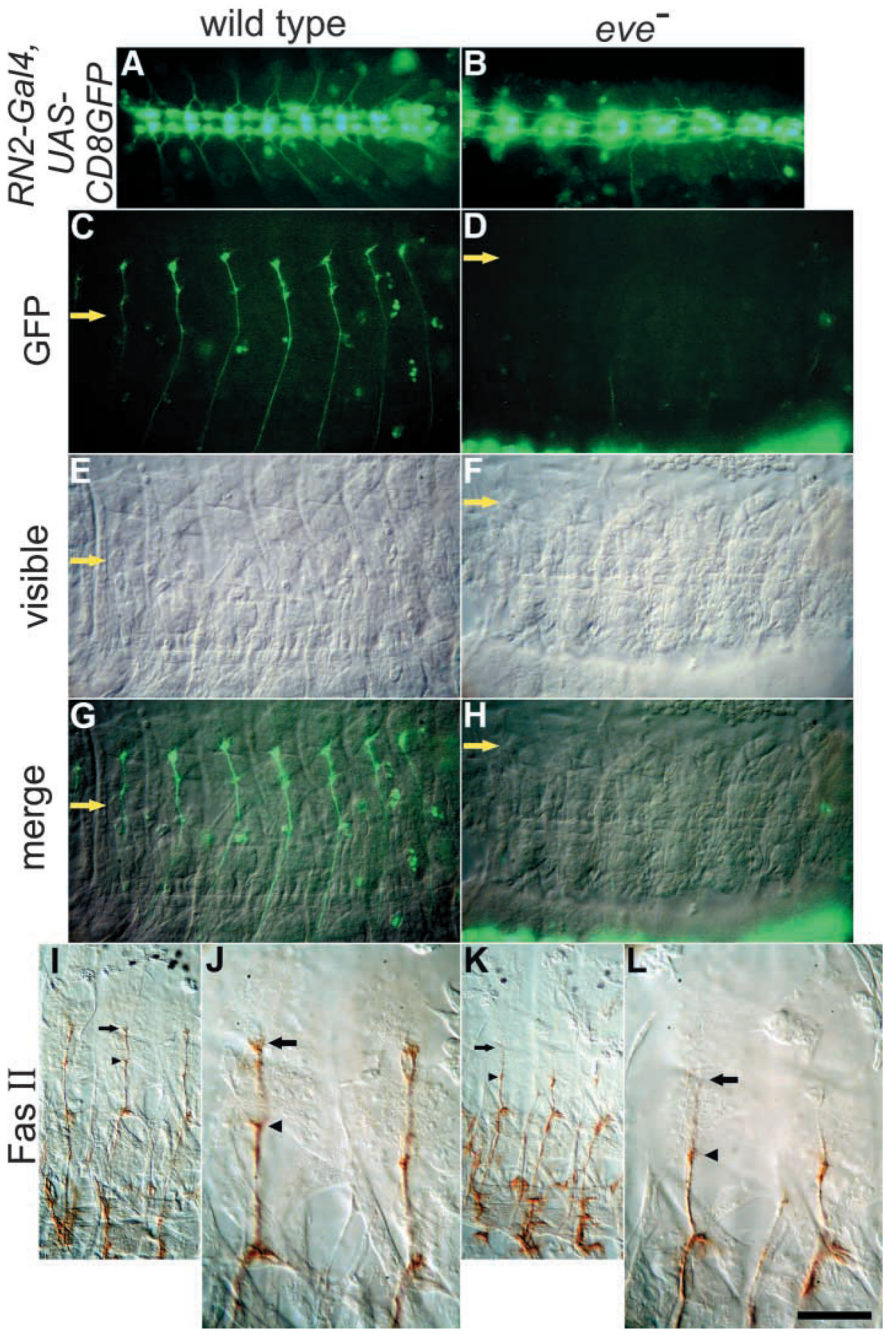

Fig. 5.

Without Eve function, most RP2 and aCC axons do not reach the muscle field. The combination of *RN2-Gal4* and *UAS-CD8GFP* transgenes (two copies each) was placed in either a wild-type (left column) or a ΔRP2A/ΔRP2C mutant background (right column). Stage 16 embryos are shown, anterior towards the left, and dorsal upwards (except A and B, which are centered on the ventral midline). (A,B) Overview of the CNS. (C,D) GFP in the muscle field. Note that in the mutant, only a few axons are visible, and that they do not reach to the dorsal muscle field. The yellow arrow indicates the same lateral position in all panels (D,F,H are a more ventral view in order to show the small amount of axonal outgrowth that occurs near the edge of the CNS). (E,F) Nomarski view of C,D, respectively. (G) Merged image of C and E. (H) Merged

image of D and F. (I–L) Anti-Fas2 staining. (J,L) Higher magnification of I,K, respectively. Note the attachment of some axons to DO2 muscles in both the wild type and the mutant (arrowheads; neuromuscular junctions to DA2 are also present, but are not visible here), but that attachments to DO1 and DA1 (only DO1 is visible here) are barely formed in the mutant (arrows). Scale bars in B and L (equal in size): 50 μm in A–I,K; 20 μm in J,L.

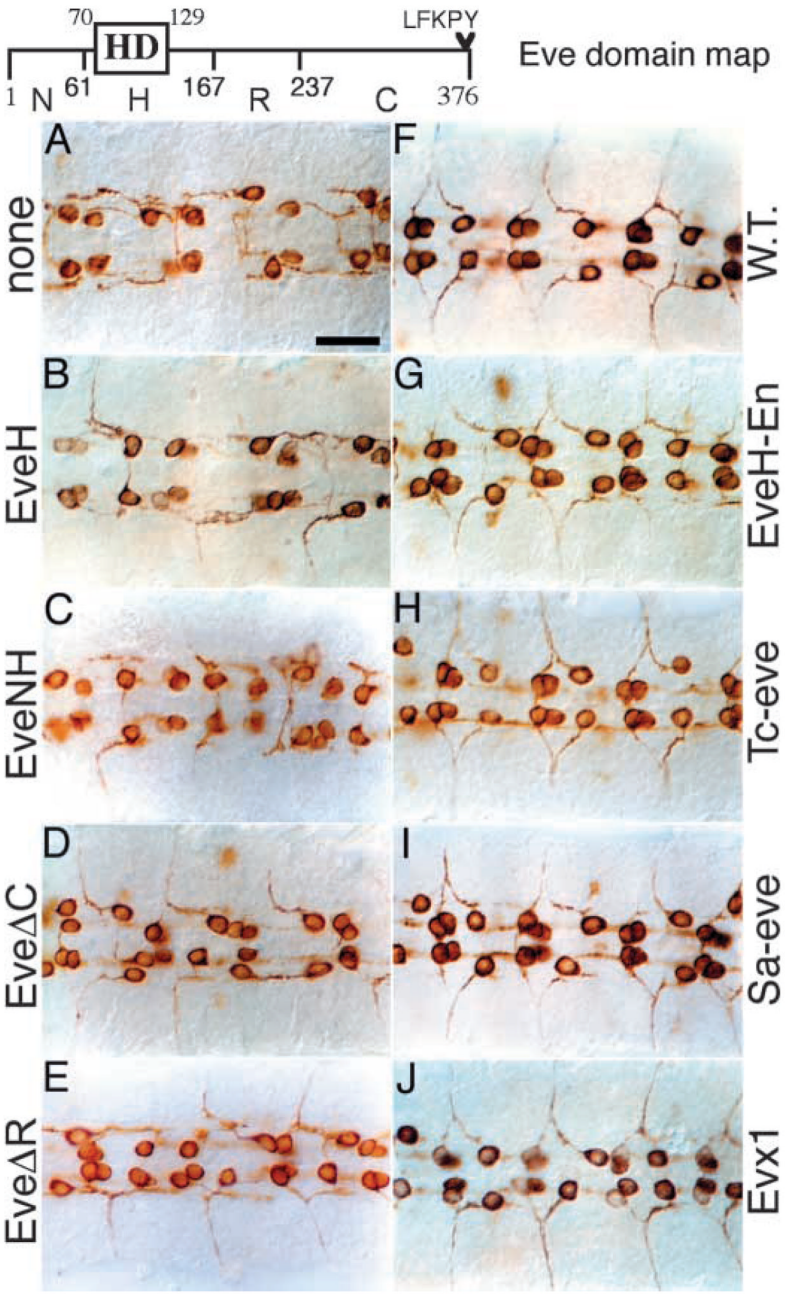

Fig. 6.

The repression function of Eve is required for normal axonal morphology. All embryos carry both the *RN2-Gal4* and *UAS-τlacZ* transgenes (marking RP2, aCC and pCC) in an RP2 mutant background, and were stained with anti-β-gal. (A) ΔRP2A/ΔRP2B (no Eve protein expressed in the marked cells). Scale bar: 20 μm. (B–J) Embryos contain in addition to the genotype in A, one copy of an *eve* transgene expressing the following modified Eve proteins: (B) Eve HD only (domain 'H' in map at top; note that there is some rescue of lateral axonal outgrowth); (C) Eve N-terminus plus HD (domains 'N' and 'H' in map; note the slight rescue, similar to B); (D) the entire Eve protein without the Groucho interaction domain ('LFKPY' in map; note the considerable but incomplete rescue); (E) the Eve protein without the Atrophin interaction

domain (‘R’ in map; note the considerable but incomplete rescue); (F) full-length Eve (note the essentially complete rescue, including cell body positioning); (G) Eve HD fused with repressor domain from En (Eve domain ‘H’ plus En amino acids 1–298; note the essentially complete rescue); (H) Tc-Eve (from *Tribolium*; note the essentially complete rescue); (I) Sa-Eve (from grasshopper; note the near-complete rescue); and (J) Evx1 (from mouse; note the near-complete rescue).

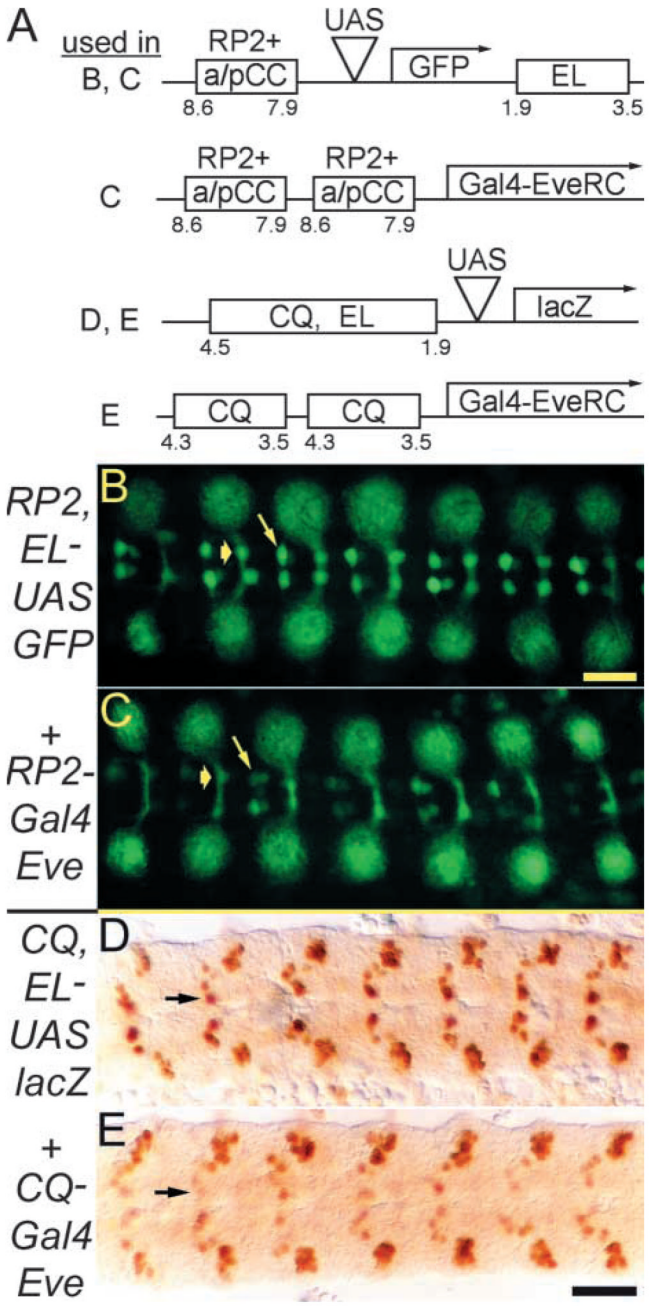

Fig. 7.

Eve exhibits active repression function in neurons. (A) The transgenes used here (see Materials and methods for details). (B) GFP expression driven by the first transgene. (C) GFP expression from the same transgene in the presence of the Gal4-EveRC repressor driven by the second transgene. Note that the intensity in RP2 (thin arrow) and a/pCC (wide arrow) is reduced compared with that in the internal control EL neurons (laterally located clusters, out of focus), where the repressor is not expressed. Yellow scale bar: 20 μm in B,C. (D) β-gal expression driven by the third transgene. (E) β-gal expression from the same transgene in the presence of the Gal4-EveRC repressor driven by the fourth transgene. Note that the intensity in U/CQ

neurons (arrow) is reduced compared with that in EL neurons, where the repressor is not expressed. Black scale bar: 20 μm in D,E.

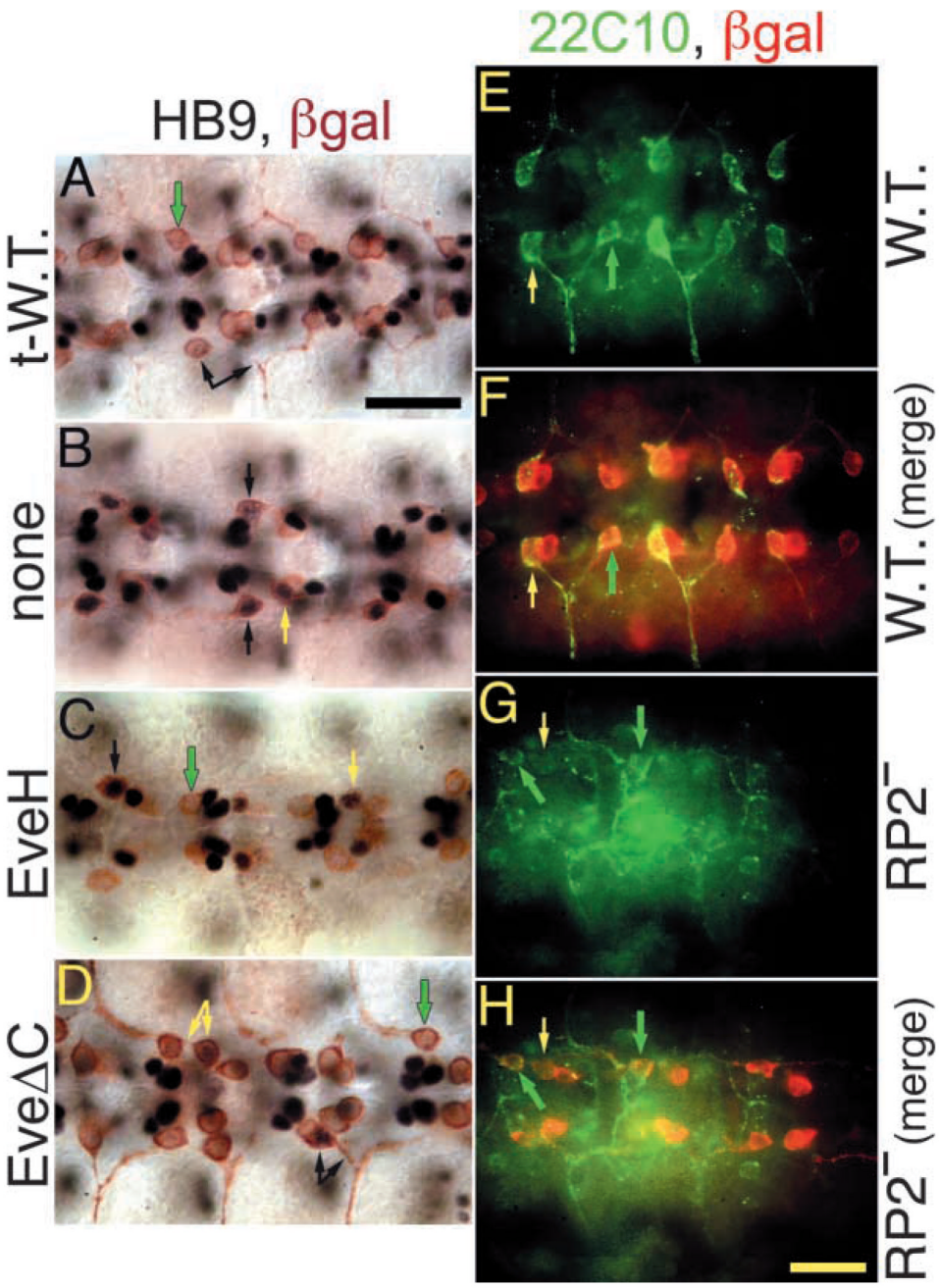

Fig. 8.

In RP2 and aCC neurons lacking *eve* function, derepression of *Drosophila* Hb9 expression correlates with mutant axonal morphology, and expression of 22C10 antigen is reduced. All embryos carry both the *RN2-Gal4* and *UAS-τlacZ* transgenes. (A–D) *Drosophila* Hb9 expression with varying degrees of rescue of the RP2 mutant; anti-Hb9 staining (black) followed by anti-β-gal staining (brown). Scale bar in A (black): 20 μm. (A) Wild-type-Eve rescued embryos. Note that Hb9 is not expressed in neurons that have a normal axonal morphology (green arrow), while RP2s that extend an axon posteriorly (abnormally) have weak Hb9 expression (arrows). (B) ΔRP2A mutant. Note that both RP2s (black arrows) and aCCs (yellow arrow) ectopically express Hb9 (although pCCs do not). (C) ΔRP2A mutant rescued

with one copy of the EveH transgene (expressing the Eve HD only, see Fig. 6C). Note that many RP2s (black arrows) and aCCs (yellow arrow) ectopically express Hb9, but some RP2s do not (green arrow). (D) ΔRP2A mutant rescued with one copy of the EveΔC transgene (expressing Eve without its Gro-dependent repressor domain, see Fig. 6D). Note that Hb9 is derepressed in the subset of neurons that show abnormal axonal phenotypes (RP2, black arrows; aCC, yellow arrows), but not in those that show a normal axonal morphology (green arrow; see text for more details). (E,F) In wild-type embryos, 22C10 antigen (green staining in E–H) is expressed in aCC (yellow arrow) and RP2 (green arrow), but not in pCC (which is immediately posterior to each aCC and stains only for β-gal, red in F; F is a merged image of 22C10 and β-gal staining, so that the overlap appears yellow, here and in H). (G,H) in the ΔRP2A mutant, expression of 22C10 antigen is reduced relative to the wild type, especially in aCC (yellow arrow), but probably also in RP2 (green arrows). Scale bar in H (yellow): 20 μm in E–H.

Table 1

Summary of RP2 phenotypes

Rescued with	*n*	RP2 axons (%)					
		Wild type* (anterior extension)	Anterior extension, truncated	Posterior extension, truncated	Posterior extension	Crossed midline	Bipolar
None 1	271	12	50	21	9	8	19
None 2	198	16	48	23	7	6	17
Wild-type Eve	278	97	0	0	1	2	0.4
t-wild-type Eve	186	78	6	6	6	4	9
t-EveH	359	29	35	15	6	15	27
t-EveNH	370	29	43	12	1	15	16
EveΔC	215	45	40	9	3	3	15
t-EveΔR	300	45	26	12	6	6	25
t-EveH-En	180	92	5	2	1	0	1
t-Tc-Eve	224	90	3	1	4	2	4
t-Sa-Eve	169	92	1	1	2	4	4
t-Evx1	183	88	6	1	3	2	7

The first column indicates the proteins expressed in RP2 neurons (in an RP2 mutant background, see text) in order to analyze their ability to rescue the *eve*-mutant phenotype.

None 1, ΔRP2A/ΔRP2A; none 2, ΔRP2A/ΔRP2B; wild-type Eve, wild-type Eve protein; t-(protein name), N-terminal Flag-tagged version of the protein (other protein names are described in the legend to Fig. 6 and in the text).

The lines none 2, t-wild-type Eve, t-EveH, t-EveNH and t-Evx1 were analyzed with one copy of the *τLacZ* marker, while the rest carried two copies of the marker. *n*, total number of axons counted. (Those neurons that showed bipolarity, extending an axon in two directions, were counted twice.)

Other columns show the percentage of neurons with the following phenotypes. Wild type* indicates a phenotype similar to that in the wild type, i.e. the axon extended anteriorly, turned laterally at the pISN and clearly extended further. However, in the unrescued lines, although these axons exited the CNS, they rarely if ever extended fully to their normal target area, the dorsal muscle field (see Fig. 5). ‘Anterior extension, truncated’ indicates extended an axon anteriorly; although many of these axons reached the pISN, they did not extend significantly further toward the muscle field. ‘Posterior extension, truncated’ indicates extended an axon posteriorly, but failed to extend significantly toward the muscle field. ‘Posterior extension’ indicates extended an axon posteriorly, which turned laterally at the aISN, and extended further, toward the muscle field. However, as with ‘wild type*’, these failed to extend to the dorsal muscle field in the unrescued lines (see Fig. 5). Crossed midline: axon crossed the midline (midline crossing did not occur in any of the previous categories); almost all of these crossed at the anterior commissure. Bipolar indicates the percentage of neurons with axons apparently extending in two directions.

Table 2

Summary of aCC phenotypes

Rescued with	*n*	aCC axons (%)					
		Wild type (posterior extension)	Posterior extension, truncated	Anterior extension	Crossed midline	No axons	Not visible
None 1	275	2	34	19	12	33	0
None 2	103	0	33	16	18	33	60
Wild-type Eve	261	100	0	0	0	0	0
t-wild-type Eve	169	93	3	2	0	2	0
t-EveH	128	2	31	17	7	43	46
t-EveNH	132	0	21	13	3	63	35
EveΔC	176	48	33	4	3	12	0
t-EveΔR	221	48	34	6	1	11	0
t-EveH-En	192	95	2	1	0	2	0
t-Tc-Eve	208	97	2	0	0	1	0
t-Sa-Eve	157	100	0	0	0	0	0
t-Evx1	157	71	7	6	8	8	5

The first two columns are as described in Table 1. Columns 3–7 show the percentage of neurons with the following phenotypes. Wild type indicates extended an axon posterolaterally, which turned at the aISN, and clearly extended further; however, in the unrescued lines, even the few in this category did not extend fully to the dorsal muscle field (see Fig. 5). ‘Posterior extension, truncated’ indicates extended an axon posteriorly, including short axons which contacted a nearby RP2 axon. ‘Anterior extension’ indicates extended an axon anteriorly, including short axons which contacted a nearby RP2 axon. ‘Crossed midline’ indicates axon crossed the midline (midline crossing did not occur in any of the other categories); the majority (>90%) of these crossed at the posterior commissure. ‘No axons’ indicates no visible axons. Owing to the necessity of using only one copy of the marker in some lines, the intensity of staining was reduced, especially that of aCC. In cases where pCC neurons were visible but not the corresponding aCC, they were counted as not visible, and were not included in the *n* (second column).

Table 3

Summary of pCC phenotypes

		pCC axons (%)	
Rescued with	***n***	**Wild type**	**Crossed midline**
None 1	234	60	40
None 2	155	67	33
Wild-type Eve	261	100	0
t-wild-type Eve	178	99	1
t-EveH	150	83	17
t-EveNH	152	96	4
EveΔC	166	100	0
t-EveΔR	155	98	2
t-EveH-En	180	100	0
t-Tc-Eve	201	100	0
t-Sa-Eve	139	100	0
t-Evx1	164	99	1

The first two columns are as described in Table 1. Wild type indicates the percentage of neurons extending axons anteriorly, without crossing the midline. Crossed midline indicates the percentage of neurons extending axons anteriorly, which crossed the midline at the anterior commissure.